C.P. No. 1140

C.P. No. 1140

MINISTRY OF AVIATION SUPPLY

AERONAUTICAL RESEARCH COUNCIL

CURRENT PAPERS

Wind Tunnel Tests at Transonic and Supersonic Speeds to Investigate the Longitudinal Stability of a Model of the AVRO 720 Aircraft

by

E. Huntley

Aerodynamics Dept., R.A.E., Bedford

LONDON: HER MAJESTY'S STATIONERY OFFICE

UDC 533.65 : 533.693.3 : 533.694.53

CP No. 1140*
May 1960

WIND TUNNEL TESTS AT TRANSONIC AND SUPERSONIC SPEEDS TO INVESTIGATE THE LONGITUDINAL STABILITY OF A MODEL OF THE AVRO 720 AIRCRAFT

by

E. Huntley
Aerodynamics Department, RAE Bedford

SUMMARY

Tests have been made in the 3ft × 3ft wind tunnel at RAE Bedford on a 1:30 scale model of the AVRO 720 aircraft to investigate the longitudinal stability characteristics at Mach numbers between 0.70 and 2.00. Additional tests were made with airbrakes attached to the rear-fuselage and with notches cut in the leading edges of the wing at 66.7% semispan.

The results show no doubtful features apart from a sharp but small transient pitch-up at lift coefficients around $C_L = 0.45$ for $M = 0.80$ and $C_L = 0.60$ for $M = 0.96$. The instability is appreciably reduced by the application of up-elevon and is almost completely eliminated by the leading edge notches. The notches, however, introduce some instability at $M = 0.99$ where none had occurred originally.

---

*Replaces RAE Technical Note Aero 2685 - ARC 22430.

CONTENTS

1 INTRODUCTION

Tests have been made in the 3ft × 3ft tunnel at RAE Bedford to investigate the longitudinal stability of a model of the AVRO 720 aircraft. This aircraft was designed to a specification for a high-altitude interceptor operating at supersonic speeds. The tests were completed shortly before the project was cancelled.

The model was 1:30 scale and was tested at transonic Mach numbers between 0.70 and 1.02 and at supersonic Mach numbers up to 2.00. Configurations tested included the basic aircraft model for a range of elevon angles, the basic model with airbrakes attached to the rear fuselage and, finally, in an attempt to eliminate undesirable pitching moment characteristics occurring at high subsonic speeds on the basic model, tests were made with notches cut in the leading edges of the wing.

2 DETAILS OF THE MODEL

A general arrangement of the basic model is shown in Fig.1 and the main dimensions are given in Table 1. The model, which was of steel construction, consisted of a triangular wing of 60° leading edge sweep combined with a body of basically circular cross sections. The wing trailing edges were swept forward 5° and the tips were cropped giving a taper ratio of 0.03 and an aspect ratio of 2.07. The wing section was RAE 101 and the thickness-chord ratio varied from 4.40% at the wing root to 5.98% at 92% semispan; the wing between these two sections was defined by straight generating lines joining equal values of x/c at the two sections. In this respect the model wing differed slightly from the full scale wing since it was designed to facilitate model manufacture without altering appreciably the aerodynamic characteristics.

The foremost 5.2 inches of the body was drooped 2.1°. The engine duct fairing on the underside of the body was represented but the intake was faired-in and flow-through was not represented. The V-shaped canopy was faired into the fin by a longitudinal spline. The fin was of similar shape to the main wing.

The aircraft has no tailplane and is controlled by the use of full span elevons which can move together as elevators or differentially as ailerons. To obtain different elevon settings on the model, grooves were machined along the hinge lines and the controls could be bent manually to the required position within a range of $\pm 10^{\circ}$ of the unbent position. In order to cover

the higher elevon angles required for supersonic speeds the rear sections of the wing, including elevons, could be removed and replaced with sections having the elevon machined at an angle of -15° to the chordal plane. Each elevon could again be bent through -10° about the hinge line to give a maximum possible setting of -25°.

The sting support for the model incorporated a five component strain gauge balance; the sixth component, axial force, was measured by an axial force balance made integral with the model.

Details of the pair of airbrakes used in certain of the tests are given in Fig.2(a). Each was pivoted about its rear edge and the blade faced forward at an angle of 62° to the body centre line. They were fastened to the rear fuselage, one on each side, with the pivot lines 1.6 inches behind the trailing edges of the wing. Details are given in Fig.2(b) of the leading edge notches which were cut in each wing, at 66.7% semispan.

3 RANGE OF TESTS

The following table gives the configurations and speed ranges covered in the tests.

Configuration	Elevon angle	Mach number range
Basic aircraft	0	0.70 to 1.02, 1.42, 1.82, 2.00
Basic aircraft	-4.7°	0.80 to 1.02
Basic aircraft	-10°	0.80 to 1.02, 1.42 and 1.82
Basic aircraft	-20°	1.42 and 1.82
Aircraft with airbrakes	0	0.80 to 1.02, 1.42 and 1.82
Aircraft with airbrakes	-10°	0.90 to 0.99, 1.42 and 1.82
Aircraft with L.E. notches	0	0.90 to 1.02

Tests at transonic speeds were made in the 36in × 27in slotted side wall section of the 3ft tunnel[1]. The transonic Mach number range usually included the following Mach numbers: 0.80, 0.90, 0.93, 0.96, 0.99 and 1.02. Tests at supersonic speeds were made in the 36in × 36in supersonic working section.

The sting incidence range was -2° to $+9^{\circ}$ at transonic speeds and -2° to $+11^{\circ}$ at supersonic speeds. Including sting deflections, these gave incidence maxima for the model of approximately 11° and 13° respectively.

The Reynolds number of the tests varied with Mach number; the values, based on mean aerodynamic chord, are shown in Fig.3 and vary from 3.7×10^6 at subsonic speeds to 2.0×10^6 at M = 2.00. In order to fix transition at the leading edges of the wing and fin, carborundum powder mixed in aluminium paint was applied to the first 10% of the local chord on top and bottom surfaces. Transition was fixed on the nose of the model using a similar roughness band half an inch wide starting one inch from the nose.

No corrections have been applied to the results for tunnel interference effects. These are believed to be negligible up to M = 0.96 but to cause slight errors in Mach number near M = 1.0. Also it is thought that, because of the absence of plenum chamber connection, the model induces a certain amount of downwash in the tunnel which is a function of the lift on the model and which can introduce an error in incidence of the order of 3 to 4%. This means that the correct lift curve slopes can be 3 to 4% greater than the values quoted for Mach numbers between 0.70 and 1.02.

From considerations of the repeatability of results and from an assessment of systematic errors (with the exception of tunnel interference effects) it is estimated that the presented data are accurate to within the following limits.

C_L	±0.006
C_D	±0.001 for α = 0, increasing to ±0.002 for $\alpha = 10^\circ$
C_m	±0.001
α	$\pm 0.02^\circ$
η	$\pm 0.1^\circ$

Drag data have been corrected for differences between the measured fuselage base pressure and free stream static pressure.

4 PRESENTATION AND DISCUSSION OF RESULTS

Pitching moments have been taken about a point $0.305\bar{c}$ behind the leading edge of the mean aerodynamic chord, this being the mean centre of gravity position of the full scale aircraft. The test results have been plotted in Figs.4 to 12 in the form of C_L vs. α, C_D vs. C_L and C_m vs. C_L curves. Figs.4 to 6 are for the basic model, Figs.7 to 9 for the model with leading

edge notches and Figs.10 to 12 for the basic model with airbrakes attached. Derived curves are presented in Figs.13 to 23. Fig.13 shows the variation with Mach number of the drag coefficient at constant lift coefficient for the model with and without airbrakes. Figs.14 and 15 give the variation with Mach number of zero incidence lift curve slope and aerodynamic centre position. Control effectiveness for the model is shown in Figs.16 and 17 and Figs.18 to 23 relate to the characteristics of the aircraft when trimmed.

4.1 Discussion of basic data

4.1.1 Basic model

In Fig.4(a), which shows C_L vs. α curves for the basic model with controls undeflected, it may be noted that at transonic speeds up to $M = 0.96$ the slope of each curve increases with incidence but that between 8^o and 10^o there is a sudden kink in the curve. There are corresponding kinks in the drag (Fig.5(a)) and pitching moment (Figs.6(a) and 6(b)) curves; in the latter case they take the form of a sharp but small transient pitch-up. No flow visualisation tests were made on this model but Sutton's airflow observations on a 55^o delta wing[2] suggest the probable main characteristics of the flow. At low incidence the flow would be expected to separate at the leading edge over the outboard part of the wing, the boundary of the separated flow being a free vortex sheet which rolls up into a discrete vortex lying across the wing. The effect on the force characteristics is to give an increase in lift beneath the vortex and a loss of lift outboard of it. The point of origin of the vortex sheet moves inboard with increasing incidence.

Taking the results for $M = 0.80$ (Figs.4(a) and 6(a)) as typical, for lift coefficients up to $C_L = 0.45$ the slope of the C_L vs. α curve increases with incidence, whilst the stability of the aircraft remains constant. The effect on pitching moment of the increase in lift (due to the separation vortex) inboard and behind the centre of gravity is more or less balanced by the loss of lift outboard and further behind the centre of gravity. At a C_L of 0.47 the pitch-up type of instability occurs, probably for one or both of two reasons. Either the forward point of origin of the vortex sheet approaches the wing apex with a corresponding increase of lift forward of the centre of gravity[2] or the vortex separates from the wing surface near the trailing edge. The latter explanation seems the more probable for three reasons. Firstly, the instability occurs very suddenly

and is consequently more likely to be associated with a separation than with a progressive change. Secondly, the instability is most marked at M = 0.96 (Fig.6(b)) where it is likely that a shock lies across the wing and which would tend to lift the vortex from the surface. Thirdly the effect is reduced by the application of up-elevon (Figs.4, 5 and 6) suggesting that it is due to a change of flow over the rear part of the wing*.

4.1.2 Effect of notches

Though the pitch-up is believed to be due primarily to separation of the vortex, it is also probable that the progressive inward movement of the forward point of origin of the vortex sheet is a contributory factor. It was thought that if this inward movement could be inhibited in some way the separation of the vortex might be delayed. To investigate this, notches were cut in the leading edges of the wing at 66.7% semispan. This position was chosen as being the most promising after analysis of results from low speed tunnel tests[3]. The results of tests on the model with leading edge notches and elevons undeflected are given in Figs.7, 8 and 9. The notches eliminate the kink in the pitching moment curve, within the incidence range of the tests, for all Mach numbers up to M = 0.96 but at the same time introduce other unsatisfactory features at M = 0.99 which were not present for the basic model. These features involve more complex, though less serious, stability changes than those occurring on the basic model since there is a hysteresis effect and the loss of stability only occurs on decreasing incidence. The reasons for this hysteresis effect are not known but apart from this the notches work satisfactorily.

Limited pressure plotting data from tests on a swept wing with notches at 65% semispan[4], indicate that the leading edge notches have effects similar to, but rather smaller than, those of fences at the same spanwise position. Haines[5] has analysed this data more thoroughly and has also discussed in detail the effect of stall fences on a 50° swept wing[6]. It appears that the effects achieved by a fence (and, presumably, a notch) are due to the modification of the outboard chordwise loading and, in particular, to the prevention of the inward movement of the apex of the leading edge vortex. Inboard of the fence, separation can occur and a second leading edge vortex can form. At

*This pitch-up tendency is unlikely to be met in straight and level flight but in a rolling manoeuvre at high altitude (with the aircraft at high incidence) it could introduce difficulties when differential movement of the elevons reduces the angle on one wing.

incidences above 10°, therefore, it is possible for there to be two part-span rolled up vortex sheets lying across the wing.

4.1.3 Effect of airbrakes

The effects of the airbrakes on the characteristics of the basic model are shown in Figs.10, 11 and 12. The lift curve slope is appreciably reduced by the addition of the airbrakes, the effect being less at supersonic than at transonic speeds. Airbrakes cause small changes in the incidence for zero lift, more so with the control deflected than undeflected. In representative conditions the change in incidence to keep C_L constant is of the order of 0.6° or less (positive or negative). The stability of the model is also reduced at all transonic Mach numbers except M = 1.02 (Fig.12) or, alternatively, the effect can be regarded mainly as a delay in the rearward movement of the aerodynamic centre position with increase in Mach number (Fig.15).

For the full scale aircraft at a given subsonic Mach number the change of trim on putting out airbrakes would be equivalent to less than 1.5° of elevator angle; at M = 1.42, however, it could be equivalent to as much as 3.5° of elevator angle.

With the exception of M = 0.96, the airbrakes have no marked effect on the instability at transonic Mach numbers at high values of C_L. At M = 0.96 the kink in the pitching moment curve is either completely eliminated or is postponed to a higher incidence beyond the range of the tests. The explanation of this could be that the airbrakes alter the position of the wing shock which is thought to contribute to the instability on the basic aircraft at this Mach number.

The effect of the airbrakes on the drag of the model can be seen in Fig.11 in which are plotted C_D vs. C_L curves for the model with and without airbrakes, and in Fig.13, in which are plotted C_D vs. M curves for $C_L = 0$ and $C_L = 0.2$. At $C_L = 0$ the airbrakes give a ΔC_D of about 0.024 at transonic speeds and about 0.029 at M = 1.82.

4.2 Lift curve slopes and aerodynamic centre positions

Figs.14(a) and (b) show the variations with Mach number of the zero incidence lift curve slope and aerodynamic centre position for both the basic model and the model with leading edge notches. $(\partial C_L/\partial\alpha)_{\alpha=0}$ for the basic model rises to a maximum of 0.059 per degree at a Mach number of 0.96. The

curve for the model with leading edge notches follows very much the same trend but with a slightly higher maximum of 0.061 per degree.

For both configurations the aerodynamic centre moves back approximately 10% of the mean aerodynamic chord on increasing Mach number from transonic to supersonic speeds. The only appreciable difference between the results from the two configurations is that the aerodynamic centre moves back at a slightly lower Mach number for the model with leading edge notches than it does for the basic model.

The effect of adding the airbrakes is to reduce $(\partial C_L/\partial\alpha)_{\alpha=0}$ for all Mach numbers and to smooth out the curve at Mach numbers just below 1.0 (Fig.15). It also postpones, to a slightly higher value of M, the rearward movement of the aerodynamic centre with increasing Mach number.

4.3 Control effectiveness

The control effectiveness for the basic model can be assessed from Figs.16(a) and (b) where $(\partial C_m/\partial\eta)_{\alpha=0}$ and $(\partial C_L/\partial\eta)_{\alpha=0}$ are plotted against Mach number. In each figure two curves are presented. The continuous line gives the slope of the C_m vs. η (or C_L vs. η) curve at $\eta = 0$ and the broken line gives the mean slope over the range $\eta = 0$ to -10^o. The value of $-(\partial C_m/\partial\eta)_{\alpha=0}$ is about 0.008 per degree at subsonic speeds falling to 0.002 at M = 1.8. The corresponding values of $(\partial C_L/\partial\eta)_{\alpha=0}$ are 0.022 per degree at subsonic speeds and 0.005 at M = 1.8.

The effect of adding the airbrakes is to produce a reduction of approximately 10% in all of these values (Fig.17).

4.4 Trim characteristics of basic aircraft

Approximate trim characteristics of the full scale aircraft have been estimated using the tunnel results but without applying any corrections to account for differences in skin friction, aeroelastic effects, engine thrust, etc.

Curves are presented in Fig.18 showing the elevon angle required to trim the aircraft (for the mean centre of gravity position at $0.305\bar{\bar{c}}$) at lift coefficients up to $C_L = 0.4$ at transonic speeds and to $C_L = 0.2$ at M = 1.82. At Mach numbers up to M = 0.93 the aircraft can be trimmed at $C_L = 0.2$ by only 2.5^o up-elevon. As the Mach number is increased to 1.02 the aerodynamic centre moves back and the elevon angle required to trim the aircraft is increased to 5.5^o. At supersonic speeds η_{TRIM} is considerably increased because of the

reduced control effectiveness and values for a trimmed lift coefficient of 0.2 are $\eta = -13^{o}$ at $M = 1.42$ and $\eta = -20^{o}$ at $M = 1.82$. The curves of η_{TRIM} vs. C_L are reasonably linear and so can be usefully summarised by the single curve, plotted in Fig.19, showing the variation of $(\partial\eta_{TRIM}/\partial C_L)_{C_L=0}$ with Mach number.

The very large increase in elevon angle to trim, with increase in Mach number, is a consequence of taking constant C_L. In actual fact, of course, much lower C_L values would be used at the higher speeds and, for example, for straight and level flight C_L would vary with Mach number in the manner shown in Fig.20(a). Fig.20(b) shows that $-\eta_{TRIM}$ would then increase by only 2.5^{o} at 25000 ft, and 3.5^{o} at 50000 ft, on increasing Mach number from 0.8 to 1.8. Figs.20(c) and (d) complete the analysis of results for straight and level flight with curves showing the variation of trim drag coefficient with Mach number and of the incidence of the trimmed aircraft. These last two figures were prepared using the curves of Fig.21 which show the lift and drag characteristics of the trimmed aircraft.

Finally the lift/drag ratios of the trimmed aircraft have been determined and plotted in Fig.22. These curves indicate maximum values of L/D of 7.7 at $M = 0.8$ decreasing to 3.3 at $M = 1.8$, the actual variation of $(L/D)_{max}$ with Mach number being as shown in Fig.23.

5 CONCLUSIONS

Tests have been made in the 3ft × 3ft wind tunnel at RAE Bedford on a 1:30 scale model of the AVRO 720 aircraft to investigate the longitudinal stability characteristics for Mach numbers between 0.7 and 2.00.

The results show no doubtful features apart from a sharp but small transient pitch up at lift coefficients around $C_L = 0.45$ for $M = 0.80$ and $C_L = 0.60$ for $M = 0.96$. The instability is appreciably reduced by the application of up-elevon and is almost completely eliminated by the use of notches cut in the leading edges of the wing at 66.7% semispan. These notches however introduce some instability at $M = 0.99$ where none had occurred originally.

The effect, on these instabilities at high C_L, of attaching airbrakes to the rear of the fuselage is small in general but at $M = 0.96$ the airbrakes either eliminate the pitch-up completely or postpone it to a higher value of C_L beyond the range of the tests. Drag increments given by the airbrakes at

$C_L = 0$ are 0.024 at transonic speeds and 0.029 at M = 1.82. The airbrakes also reduce the lift curve slope, changes of incidence of the order of 0.6^o being necessary to maintain a constant C_L value in a representative condition.

The zero incidence lift curve slope for the basic model has a maximum of 0.059 per degree at M = 0.96. It is only slightly affected by the leading edge notches but is reduced to 0.050 per degree by the addition of the airbrakes. The aerodynamic centre for all configurations moves back approximately 10% of the mean aerodynamic chord on going from subsonic to supersonic speeds; compared with the basic model case it starts moving back at a slightly lower Mach number with notches in the leading edges and at a slightly higher Mach number with airbrakes fitted.

Values for the control effectiveness of the basic model are $-(\partial C_m/\partial \eta)_{\alpha=0}$ = 0.008 per degree at M = 0.8 decreasing to 0.002 at M = 1.8 and $(\partial C_L/\partial \eta)_{\alpha=0}$ = 0.022 per degree at M = 0.8 decreasing to 0.005 at M = 1.8. With airbrakes on these values are all reduced by approximately 10%.

Table 1

MAIN DIMENSIONS OF MODEL AND FULL SCALE AIRCRAFT

	Model scale	Full scale
Wing		
Span	10.92 inches	27.30 ft
Centre-line chord	10.24 inches	25.60 ft
Tip chord	0.31 inch	0.77 ft
Mean aerodynamic chord	6.828 inches	17.07 ft
Distance of m.a.c. from body centre line	1.876 inches	4.69 ft
Gross wing area	57.60 sq inches	360.0 sq ft
Wing section	RAE 101	
Thickness-chord ratio at 17.1%s	4.40%	4.19%
Thickness-chord ratio at 92%s	5.98%	5.51%
Taper ratio	0.03	
Aspect ratio	2.07	
L.E. sweep	60°	
T.E. sweep	-5°	
Dihedral	0	
Incidence relative to body centre line	1°	
Elevons		
Root chord	0.917 inch	2.29 ft
Total area	6.62 sq inches	41.4 sq ft
Hinge line sweep	0	
Section	Flat sides. T.E. thickness equal to ½ × H.L. thickness	
Body		
Overall length	17.25 inches	43.13 ft
Max. diameter	1.866 inches	4.67 ft
Nose droop	2.1°	
Length of drooped nose	5.20 inches	13.00 ft
Fin		
Height (from body centre-line)	3.25 inches	8.13 ft
Centre line chord	6.00 inches	15.00 ft
Root chord	4.35 inches	10.88 ft
Tip chord	0.09 inch	0.23 ft
Gross fin area	9.89 sq inches	61.8 sq ft
Fin section	RAE 101	
Thickness-chord ratio	5%	
Taper ratio	0.02	
Aspect ratio	2.14	
L.E. sweep	60°	
T.E. sweep	-5°	
Centre of gravity position		
(i) Aft of wing apex	5.332 inches	13.33 ft
(ii) Aft of L.E. of m.a.c.	0.305 × m.a.c.	

SYMBOLS

C_L	lift coefficient
C_D	drag coefficient
C_m	pitching moment coefficient (based on $\bar{\bar{c}}$)
m	pitching moment about aircraft centre of gravity ($0.305\bar{\bar{c}}$ from leading edge of m.a.c.)
S	gross wing area
$\bar{\bar{c}}$	mean aerodynamic chord
q	dynamic pressure
M	Mach number
x	streamwise distance from wing leading edge
α	body incidence
η	elevon angle (positive with T.E. down)

REFERENCES

No.	Author(s)	Title, etc.
1	E.P. Sutton	The development of slotted working section liners for transonic operation of the N.A.E. 3-foot wind tunnel. ARC R&M 3085, March 1955
2	E.P. Sutton	Some observations of the flow over a delta-winged model with 55° leading edge sweep at Mach numbers between 0.4 and 1.8. ARC R&M 3190, November 1955
3		720 aircraft. The effect of leading edge notches on longitudinal stability. AVRO W.T. Report 720/19, June 1954
4	R.E. Kuhn J.W. Wiggins A.L. Byrnes	Wind-tunnel investigation of the effect of a fence and a leading-edge notch on the aerodynamic loading characteristics in pitch of a 45° sweptback wing at high subsonic speeds. NACA RM L 53 H 24. NACA/TIB/3927, October 1953
5	A.B. Haines	Some effects of a stall fence and leading-edge notch on the pressures over a thin swept wing. (Analysis of results from NACA RM L 53 H 24.) RAE Technical Note Aero 2313 (ARC 17146) (1954)
6	A.B. Haines C.W. Rhodes	Tests in the R.A.E. 10 ft × 7 ft high speed tunnel on a 7.5% thick, 50° swept wing fitted with stall fences and a leading-edge chord-extension. ARC R&M 3043, September 1954
7	J.W. Wiggins	Wind tunnel investigation at high subsonic speeds of the static longitudinal and static lateral stability characteristics of a wing-fuselage combination having a triangular wing of aspect ratio 2.31 and an NACA 65A003 airfoil. NACA RM L 53 G 09a. NACA/TIB/3886, August 1953

ATTACHED:

Drgs: 39501s to 39533s

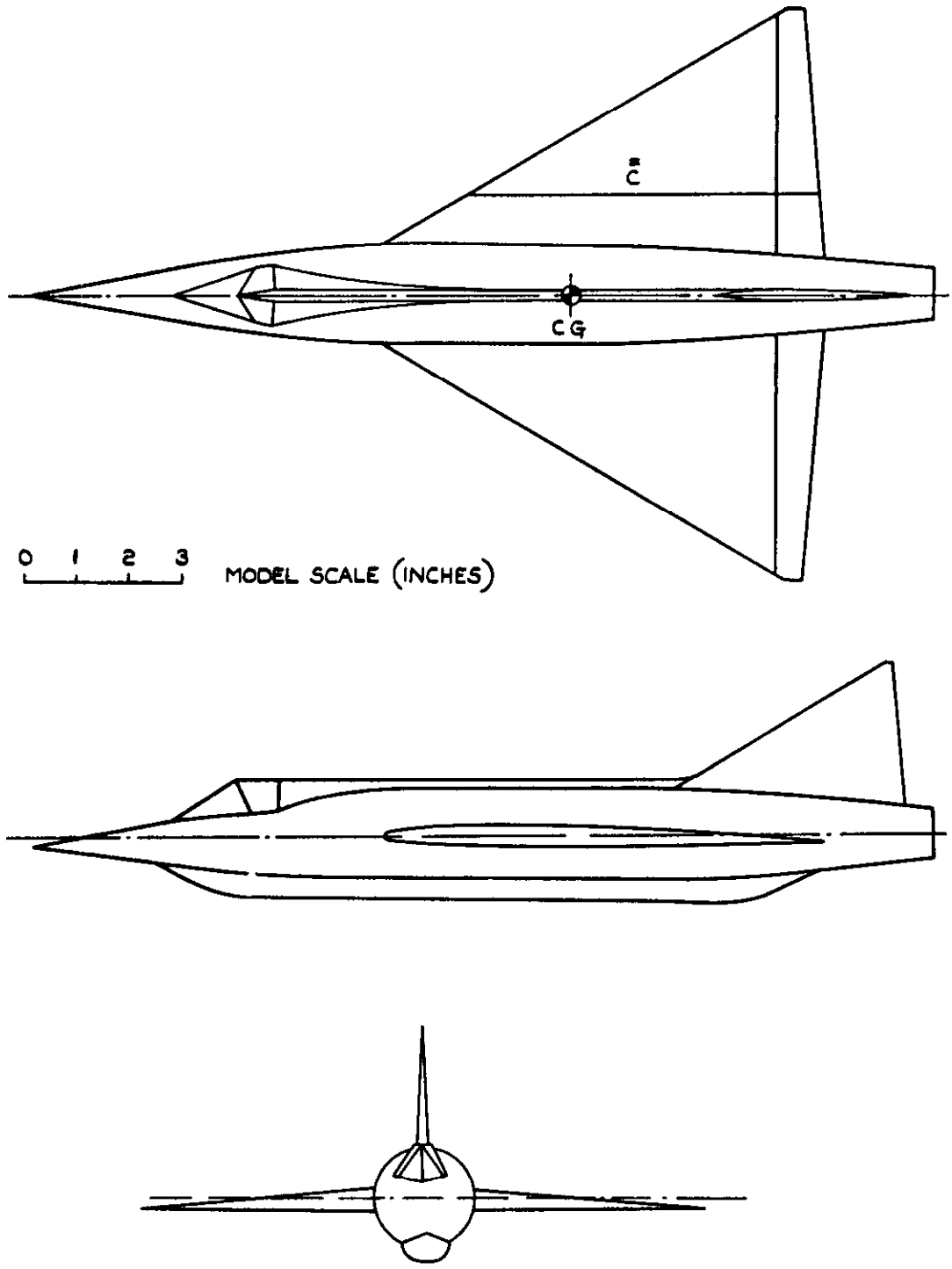

FIG. I. GENERAL ARRANGEMENT OF MODEL OF BASIC AIRCRAFT.

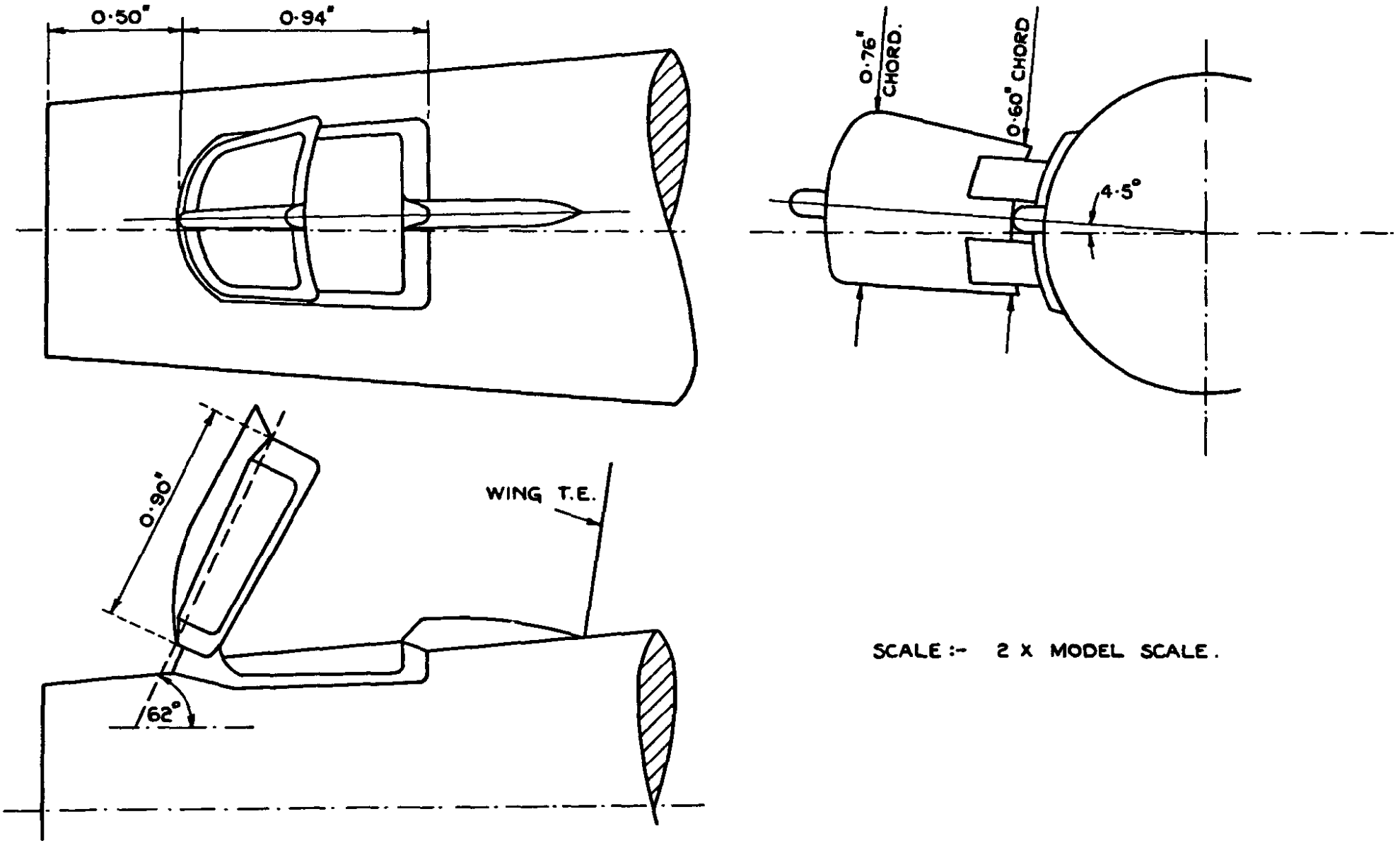

FIG. 2(a). DETAILS OF AIRBRAKES.

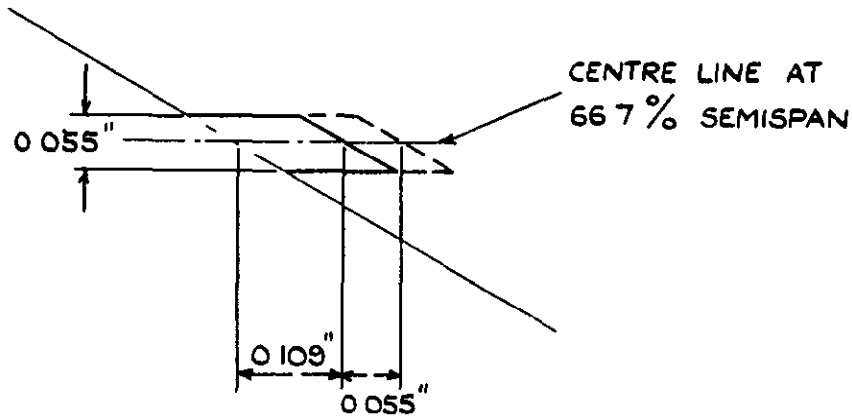

SCALE - 5 x MODEL SCALE

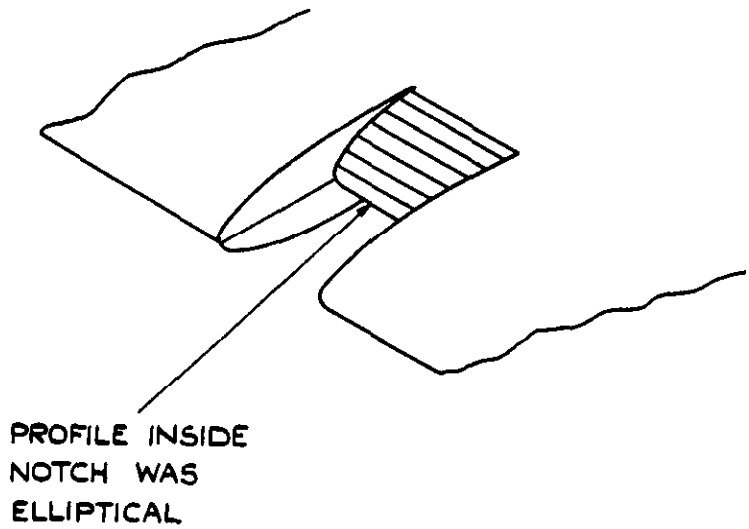

FIG.2(b) DETAILS OF LEADING EDGE NOTCHES.

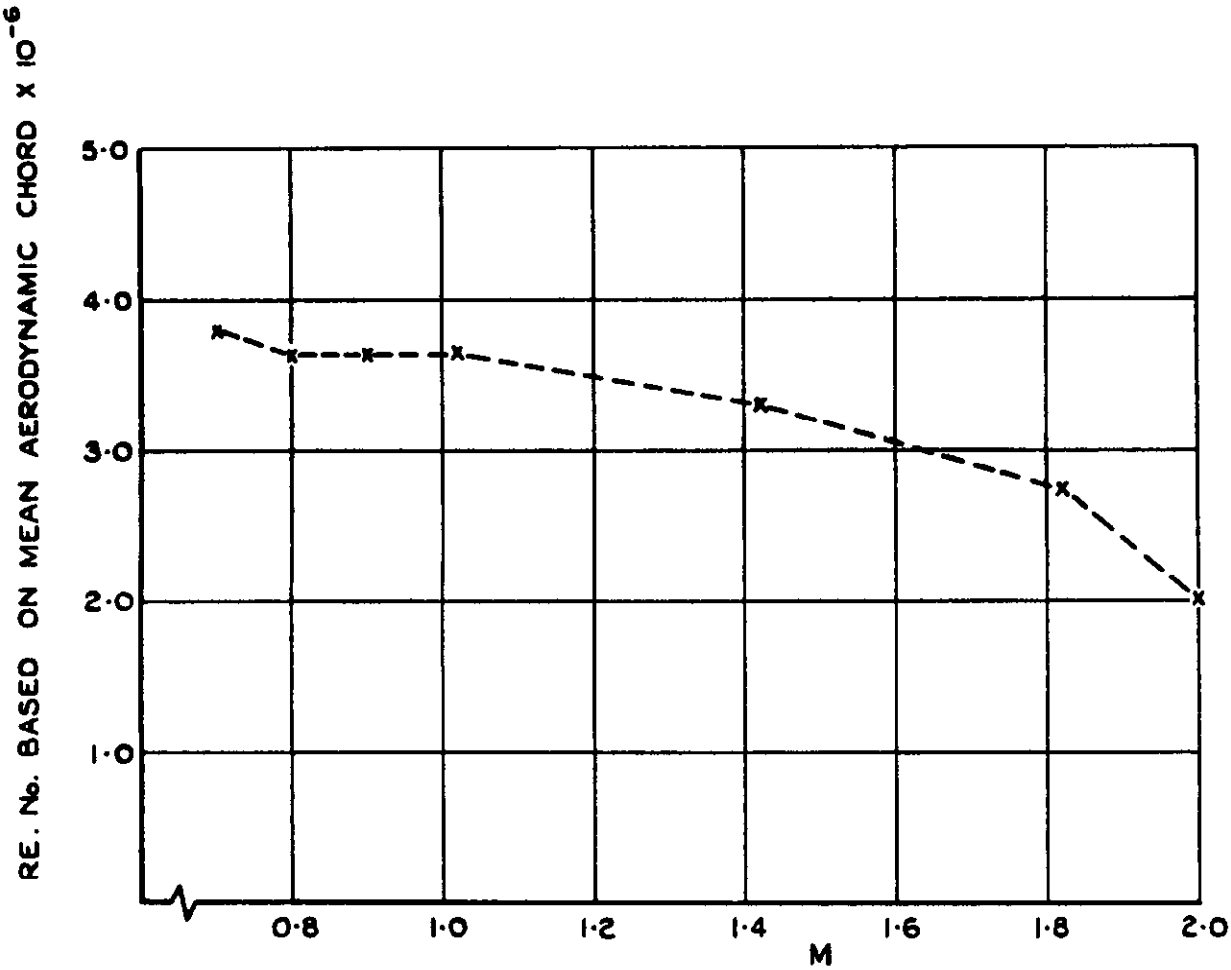

FIG. 3. VARIATION OF TEST REYNOLDS NUMBER WITH MACH NUMBER.

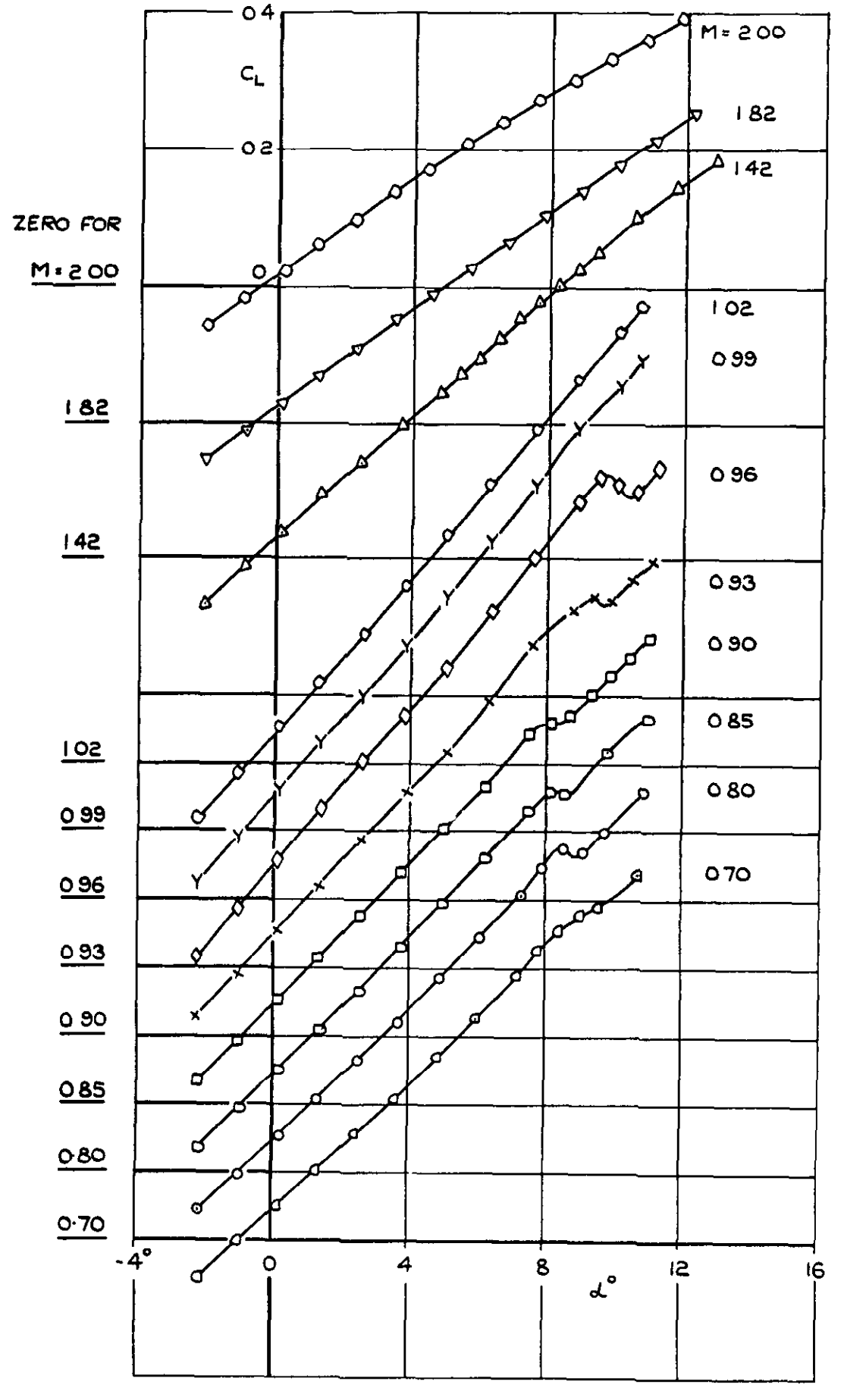

FIG. 4(a) VARIATION OF C_L WITH α FOR BASIC MODEL; $\eta = 0$.

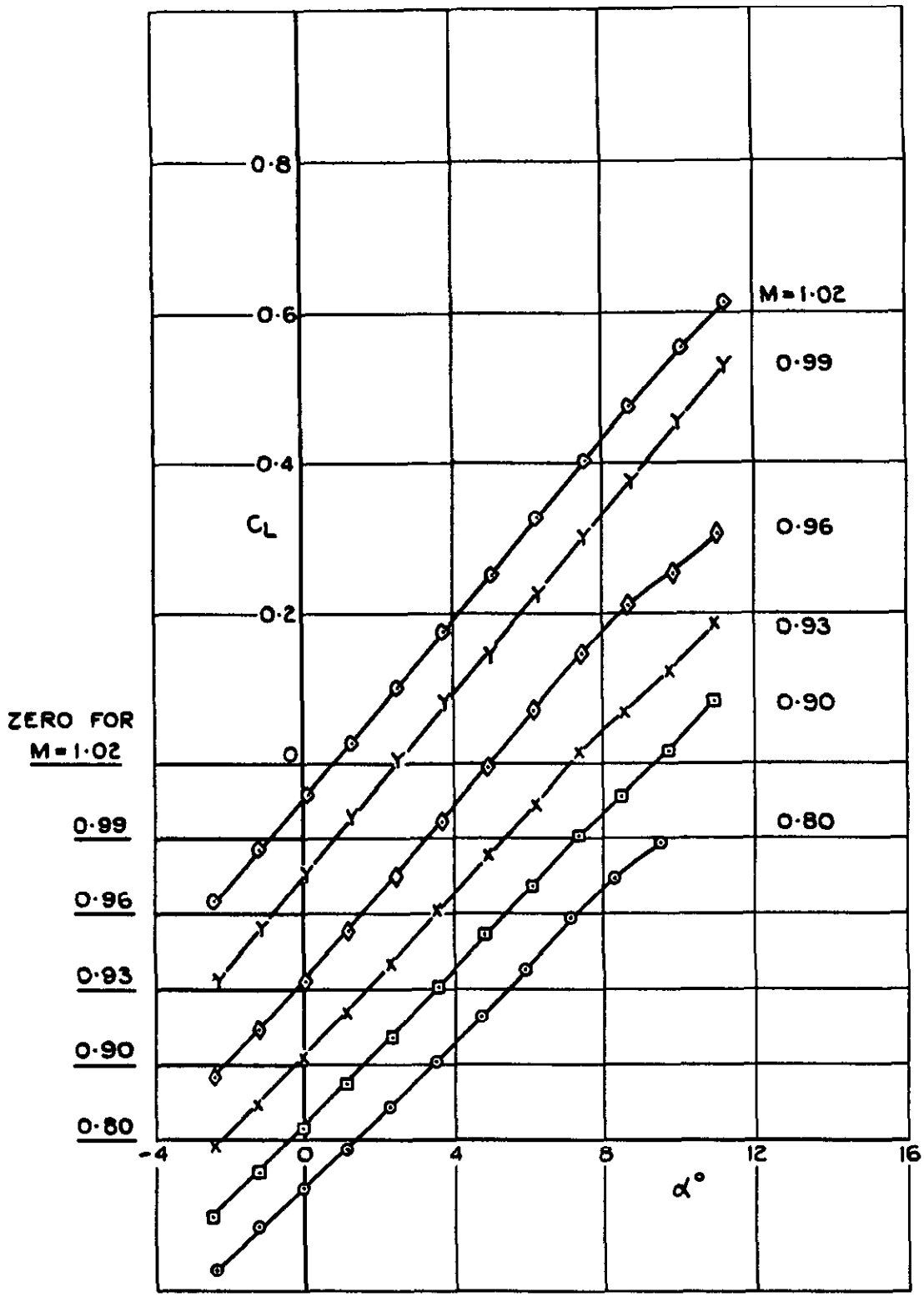

FIG.4(b)VARIATION OF C_L WITH α FOR BASIC MODEL ; $\eta = -4{\cdot}7^\circ$.

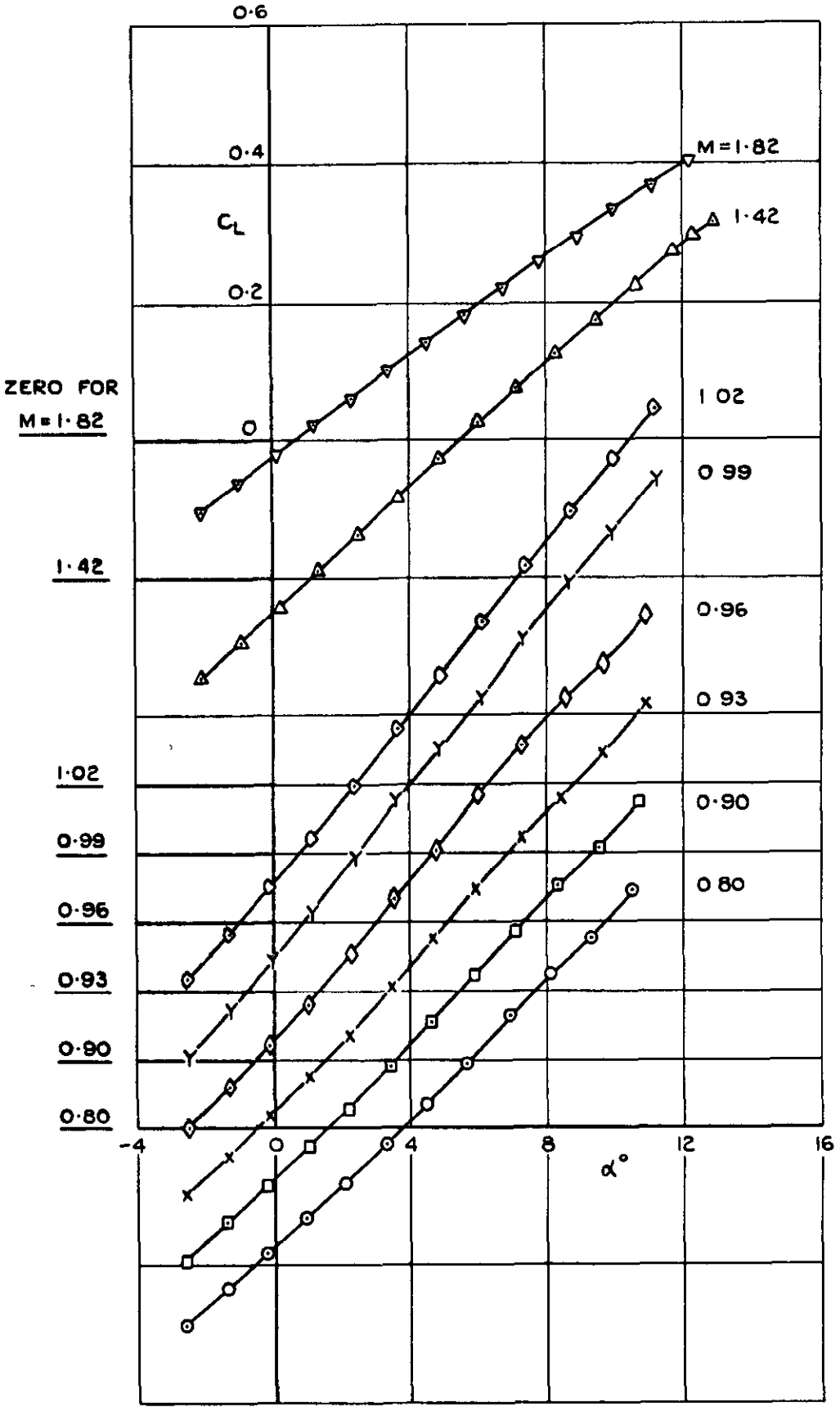

FIG. 4(c) VARIATION OF C_L WITH α FOR BASIC MODEL ; $\eta = -10^{\circ}$.

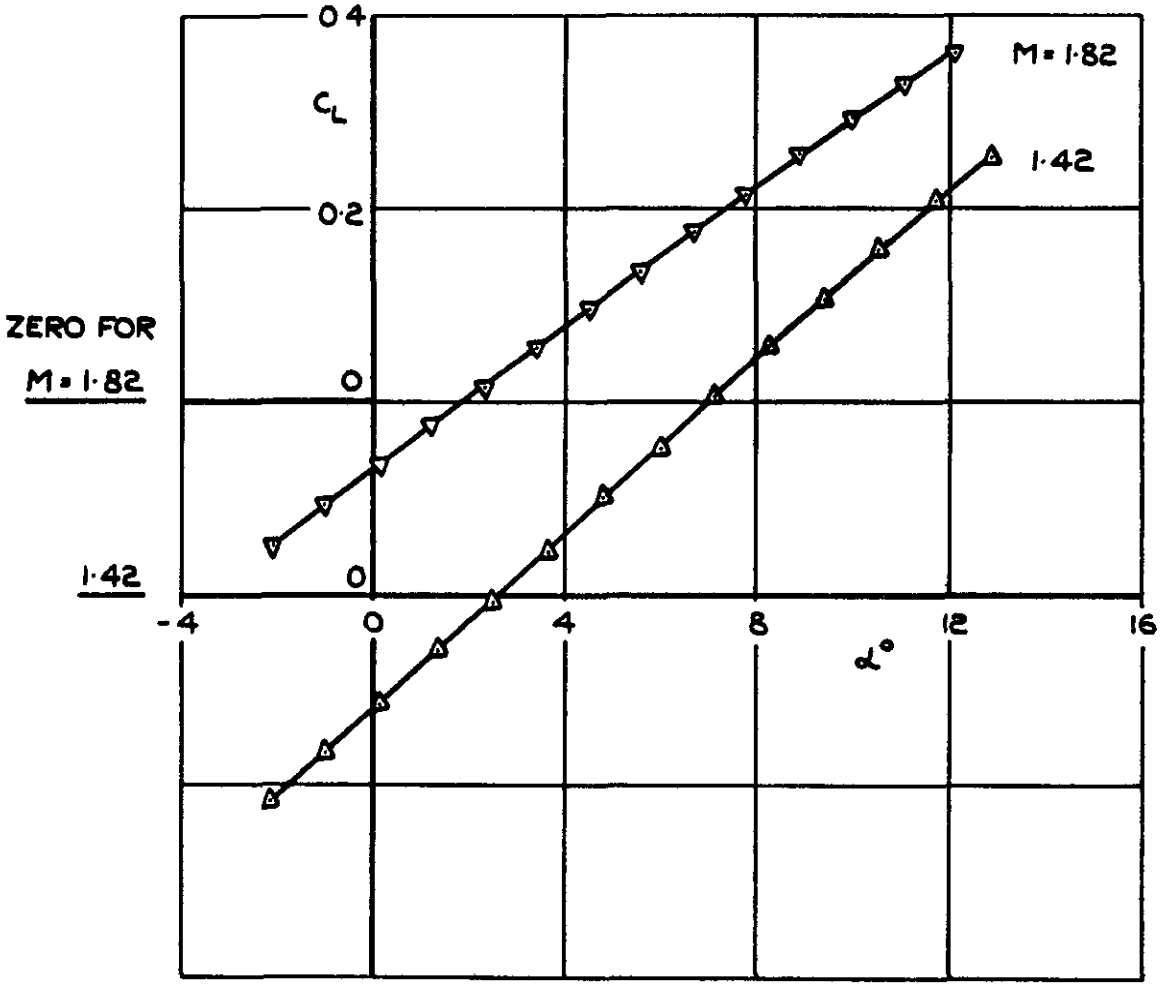

FIG.4(d) VARIATION OF C_L WITH α FOR BASIC MODEL; $\eta = -20°$.

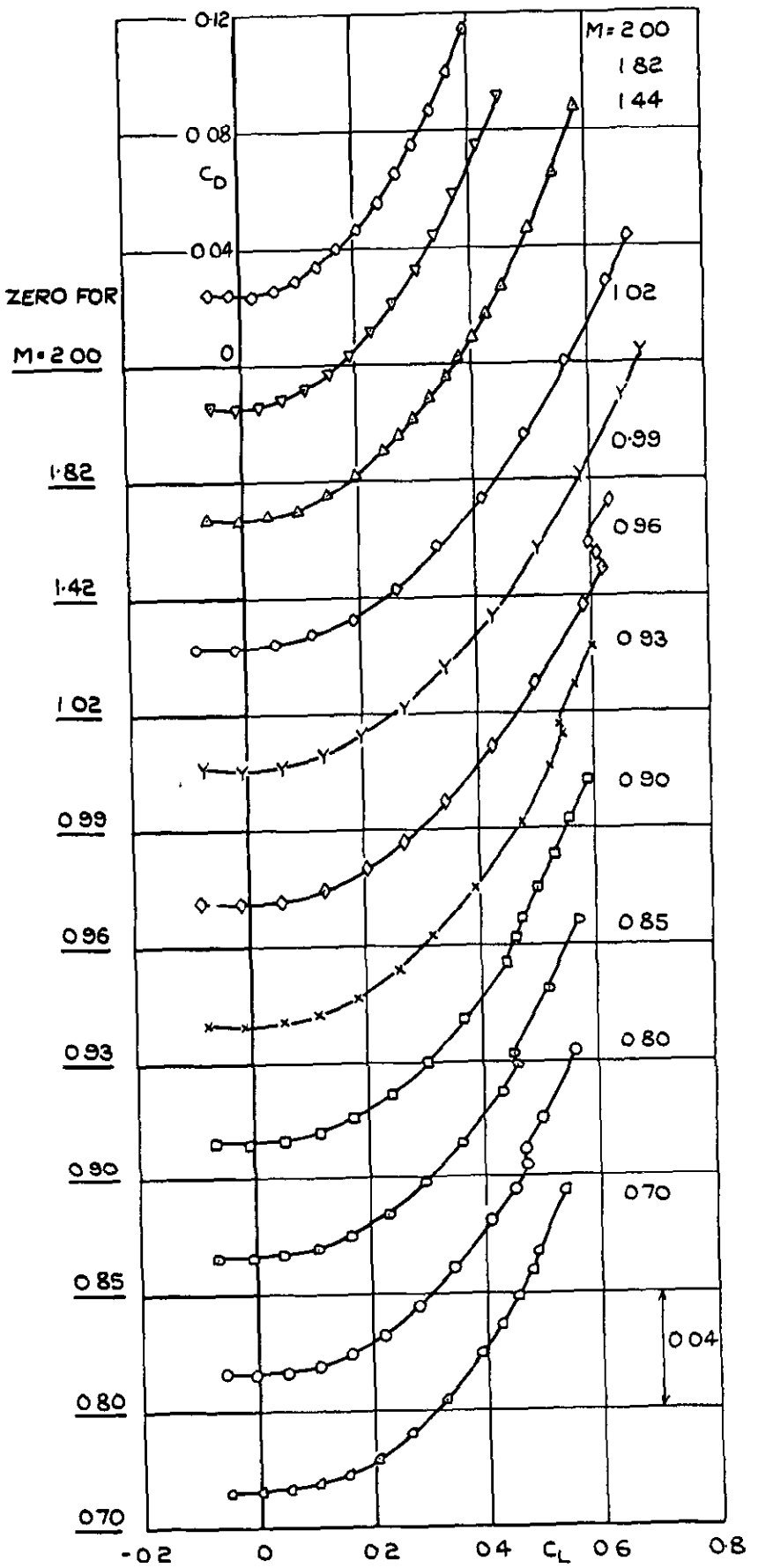

FIG.5(a) VARIATION OF C_D WITH C_L FOR BASIC MODEL ; $\eta = 0$.

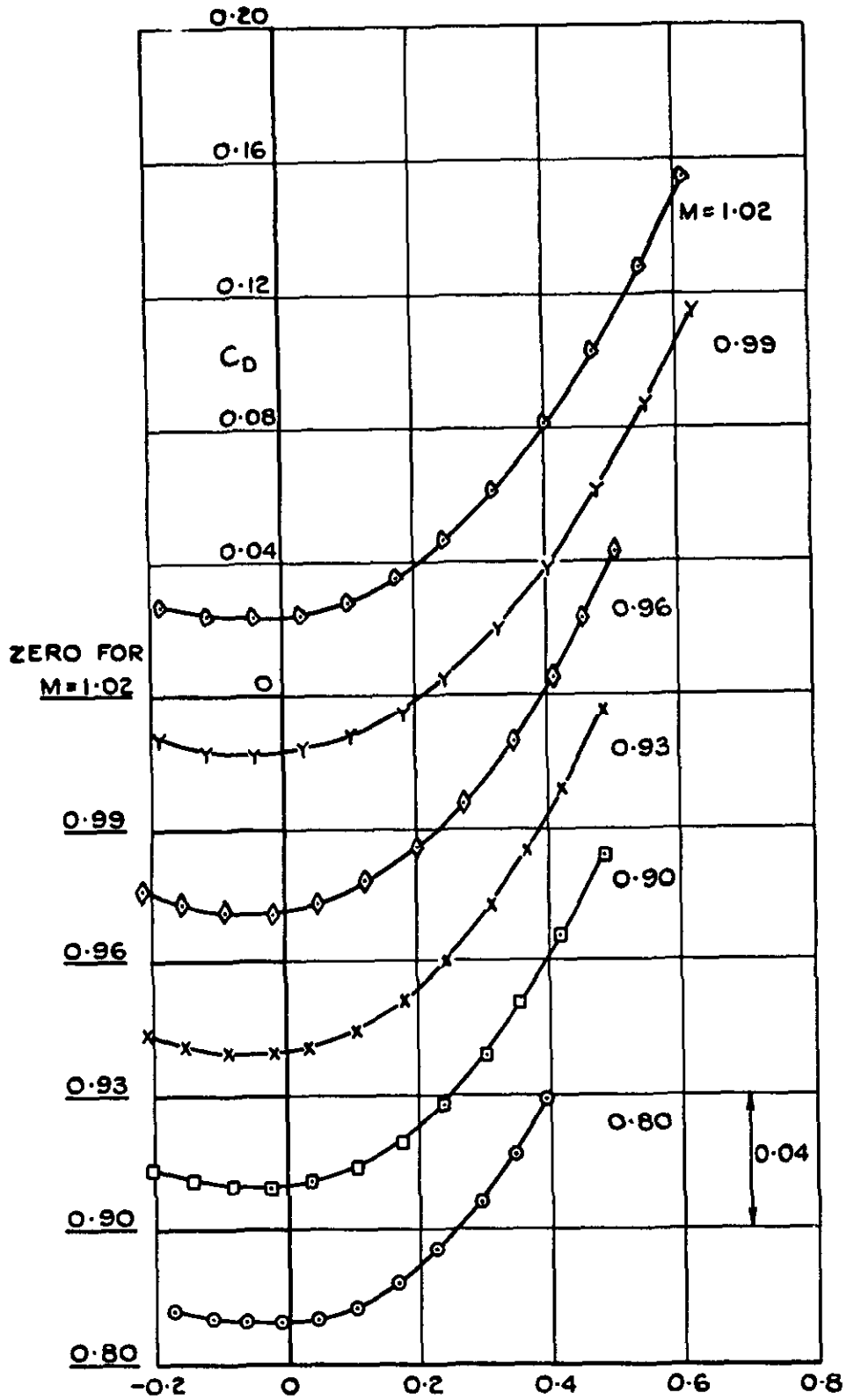

FIG.5(b)VARIATION OF C_D WITH C_L FOR BASIC MODEL ; $\eta = -4{\cdot}7^{\circ}$.

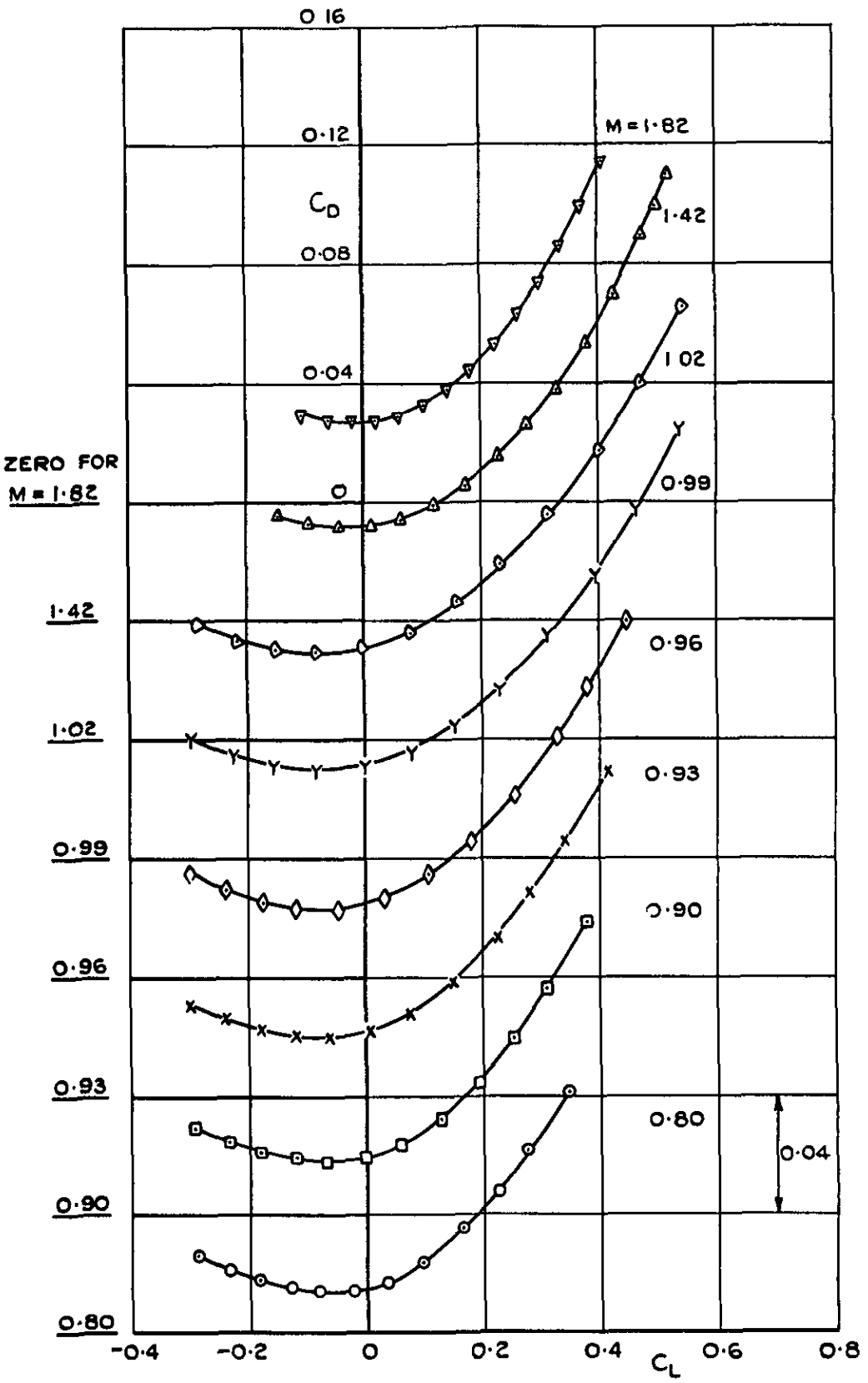

FIG.5(c). VARIATION OF C_D WITH C_L FOR BASIC MODEL ; $\eta = -10^\circ$.

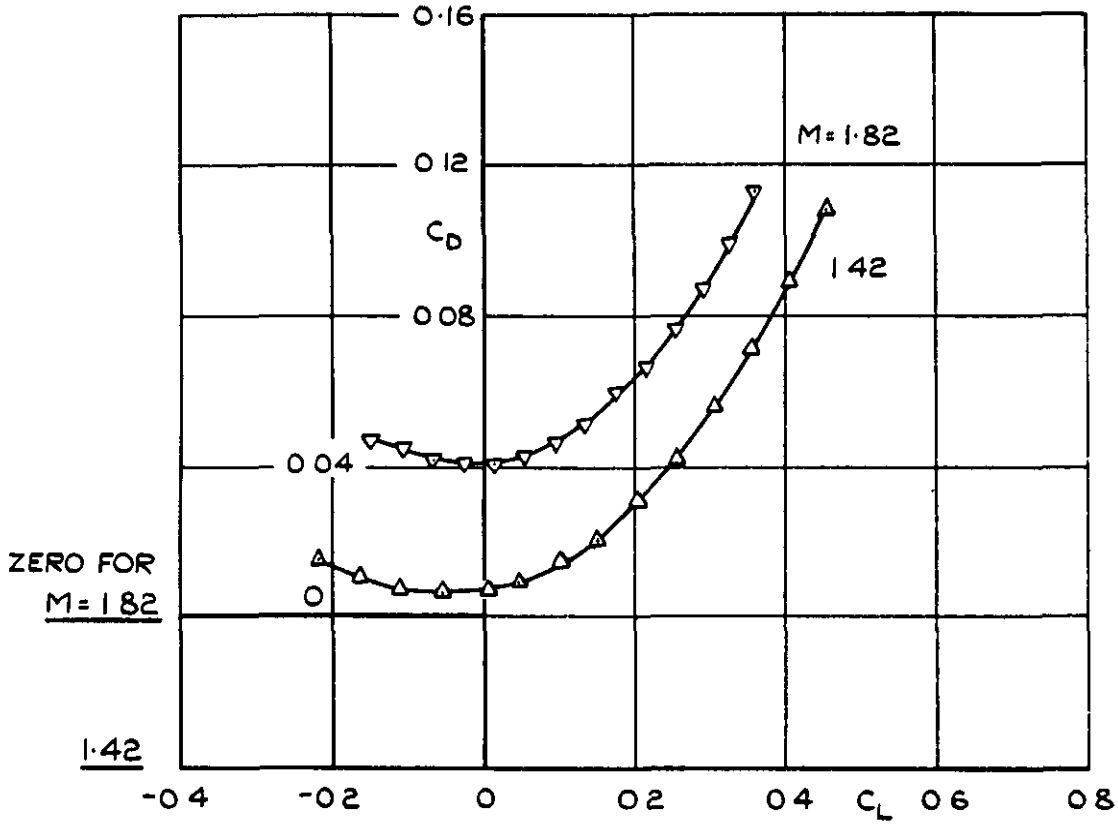

FIG.5(d) VARIATION OF C_D WITH C_L FOR BASIC MODEL; $\eta = -20°$.

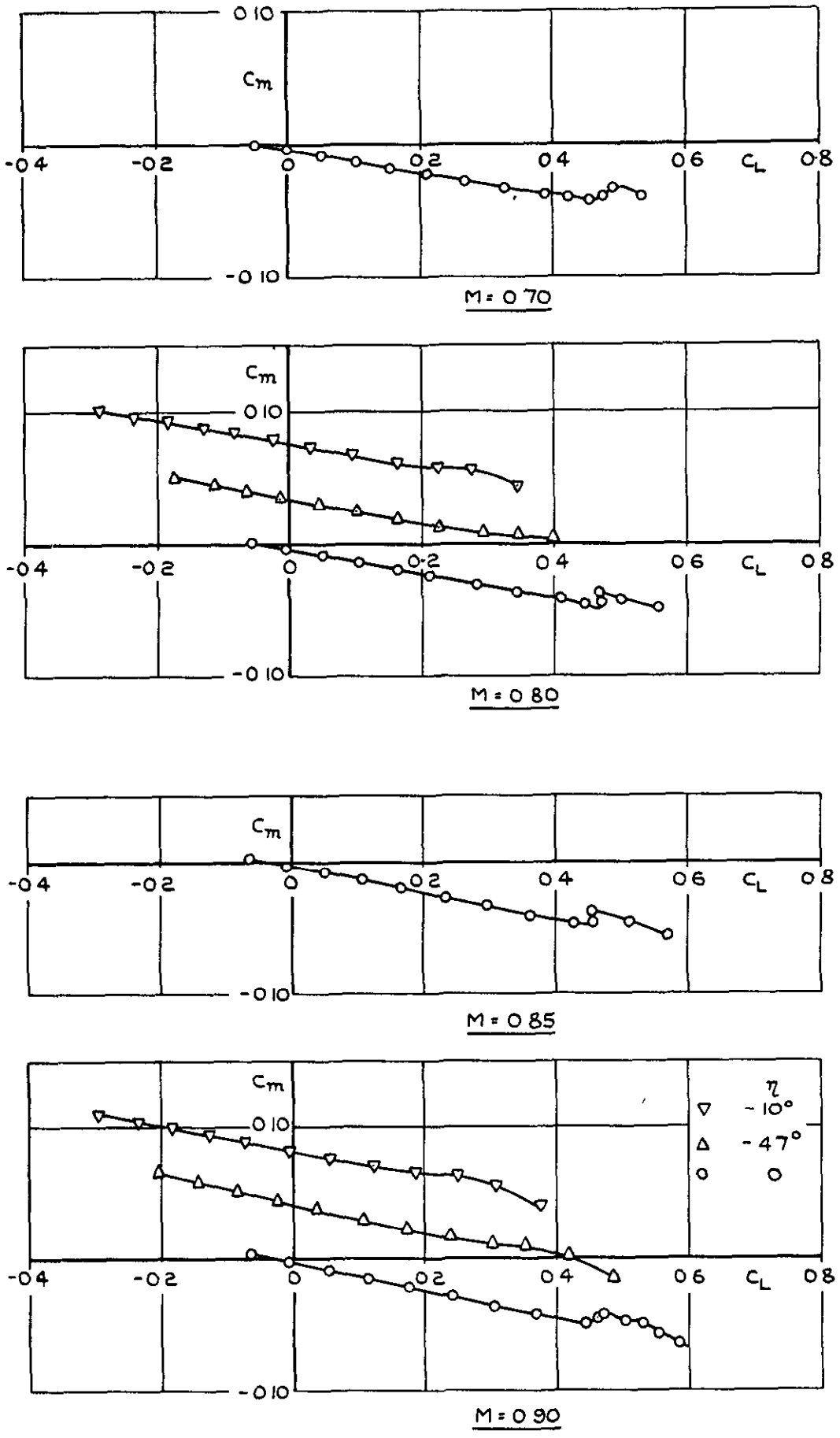

FIG. 6. VARIATION OF C_m WITH C_L FOR BASIC MODEL WITH VARIOUS ELEVON ANGLES

(a) M = 0·70 TO 0·90

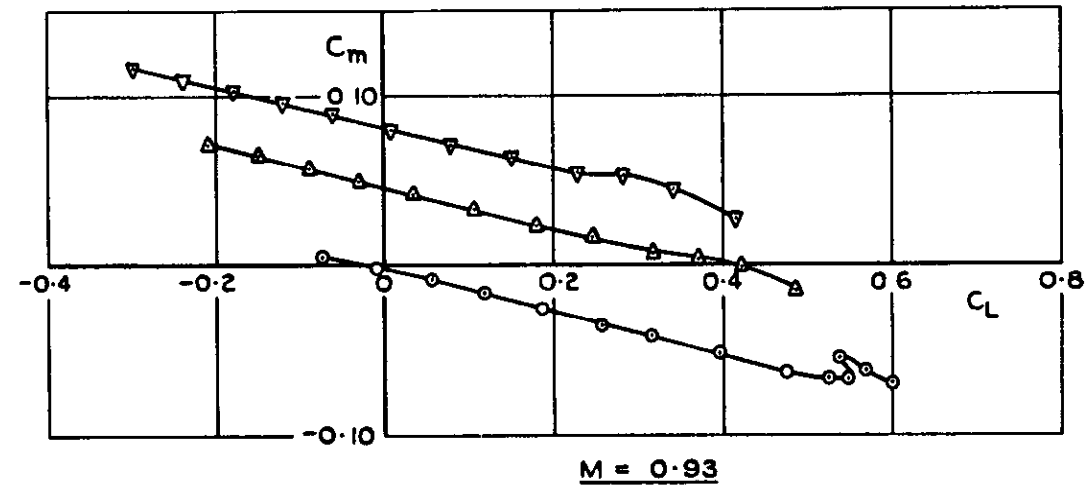

M = 0·93

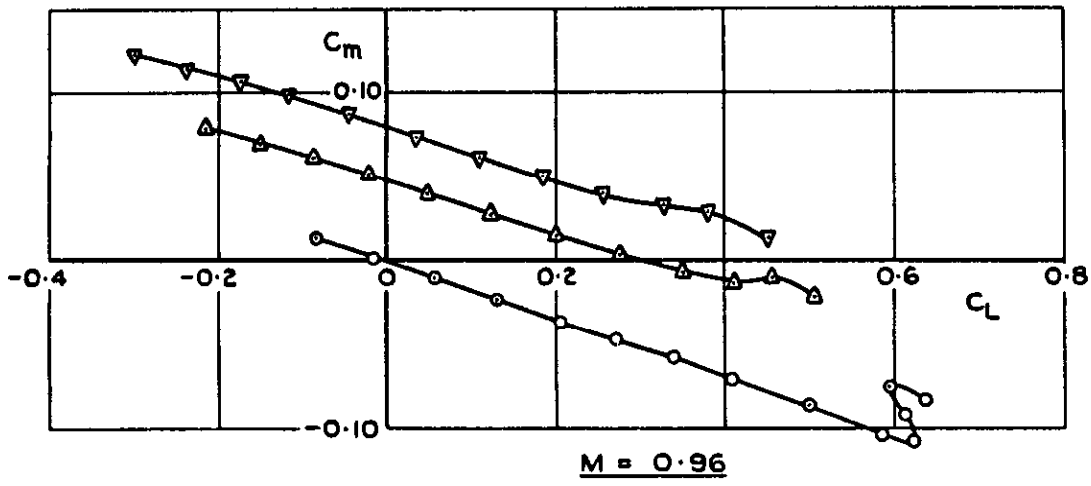

M = 0·96

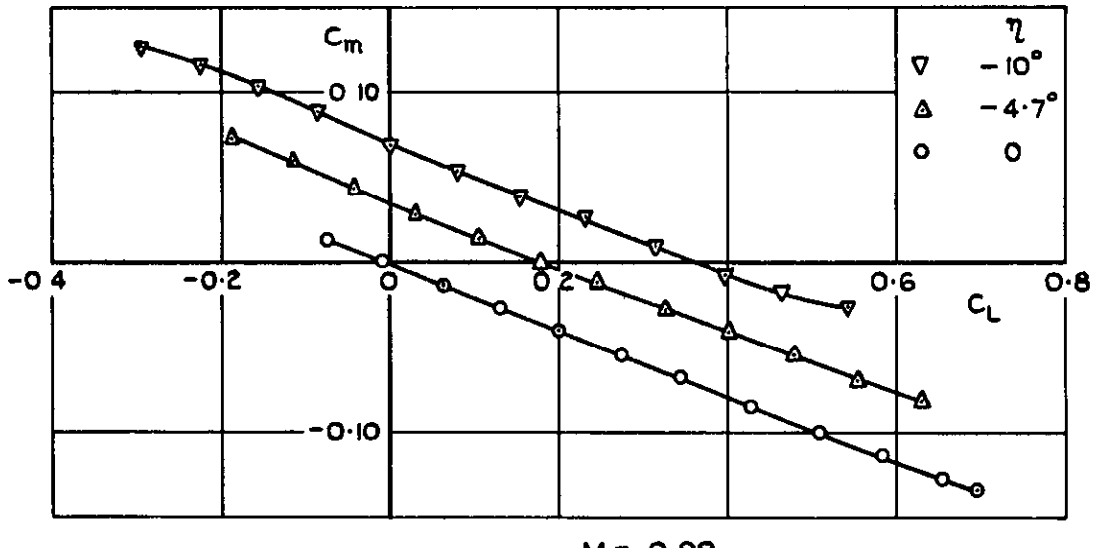

M = 0·99

FIG. 6. VARIATION OF C_m WITH C_L FOR BASIC MODEL WITH VARIOUS ELEVON ANGLES.

(b) M = 0·93 TO 0·99.

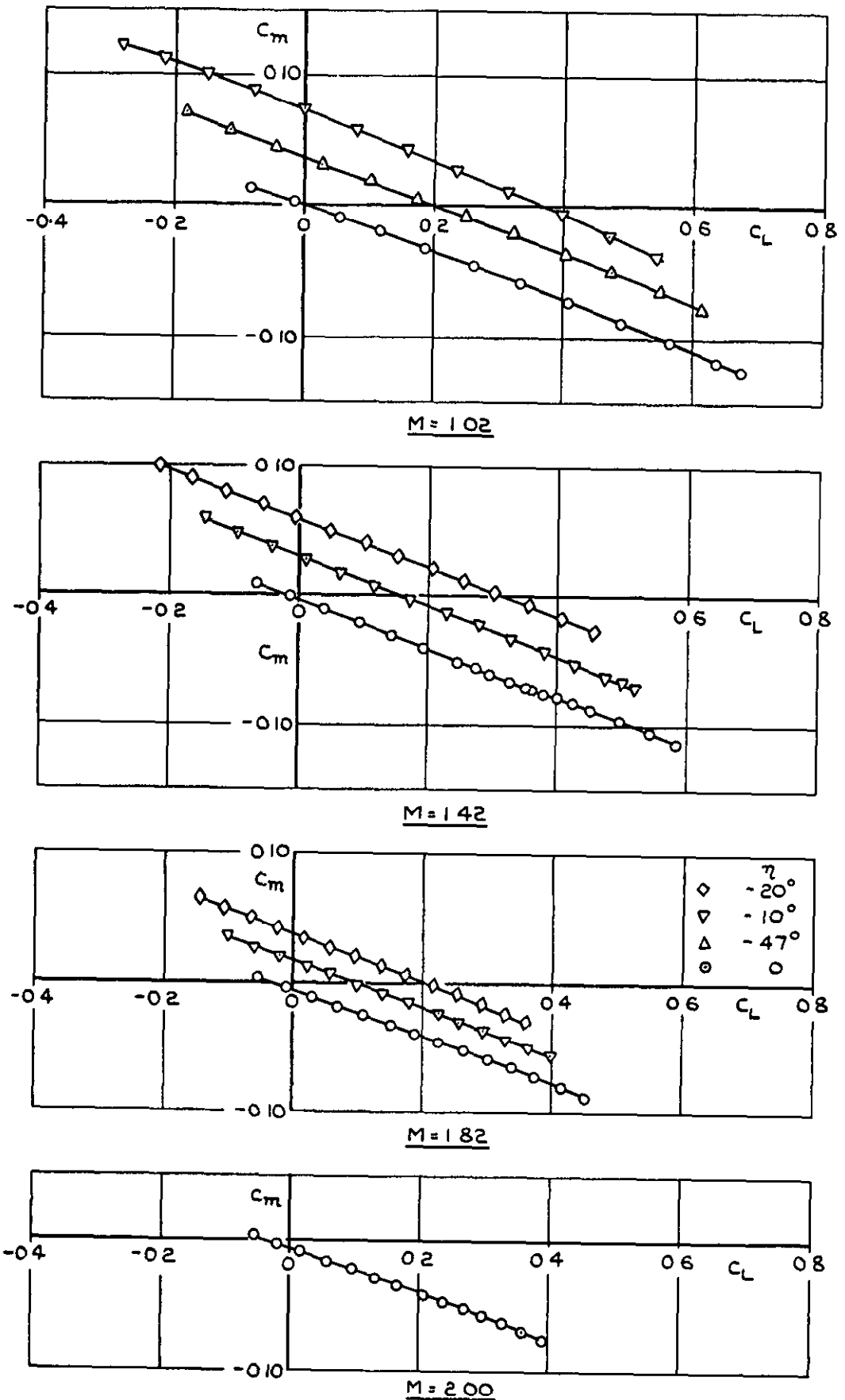

FIG. 6. VARIATION OF C_m WITH C_L FOR BASIC MODEL WITH VARIOUS ELEVON ANGLES

(c) M = 1·02 TO 2·00

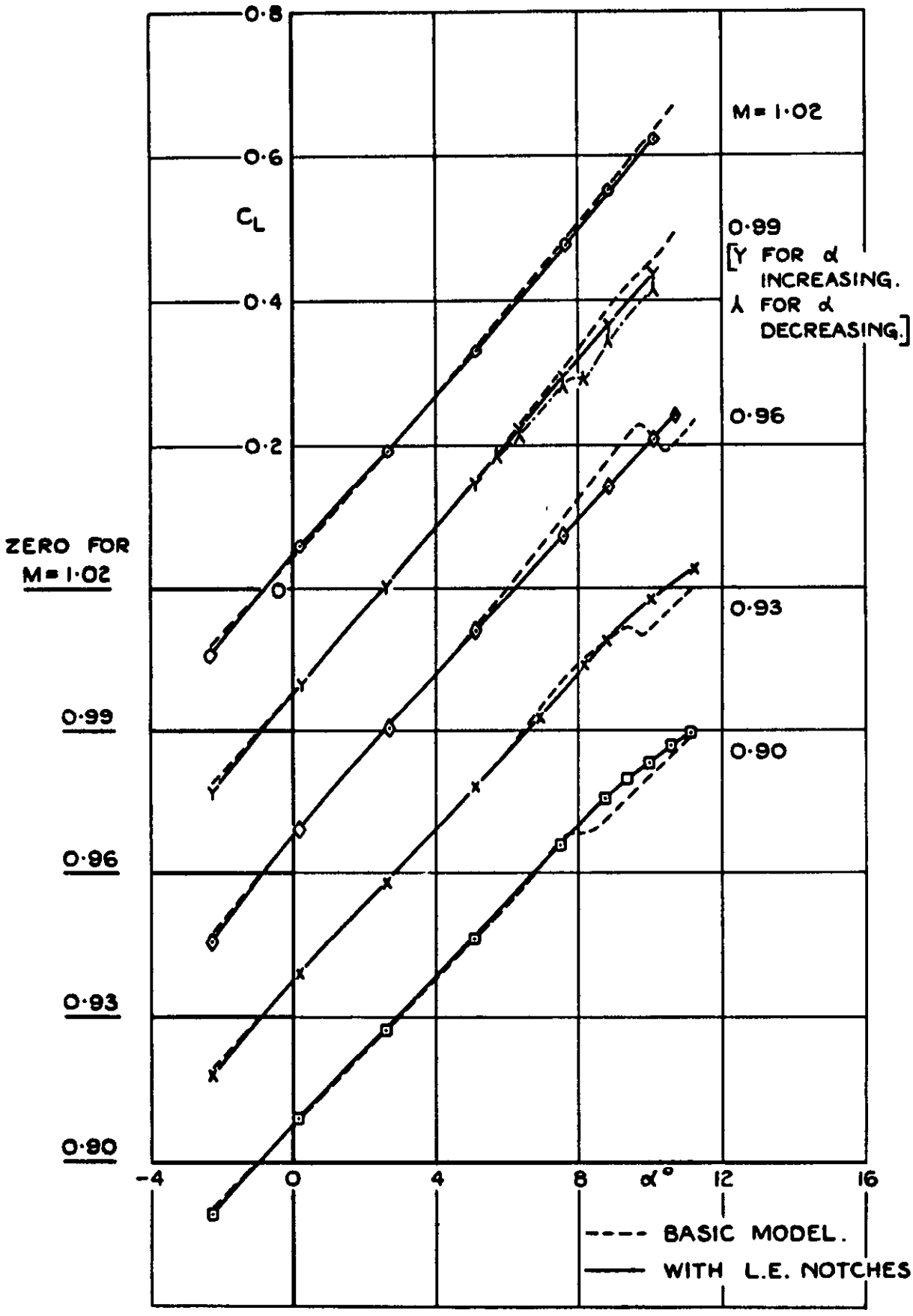

FIG. 7. VARIATION OF C_L WITH α FOR MODEL WITH LEADING EDGE NOTCHES; $\eta = 0$.

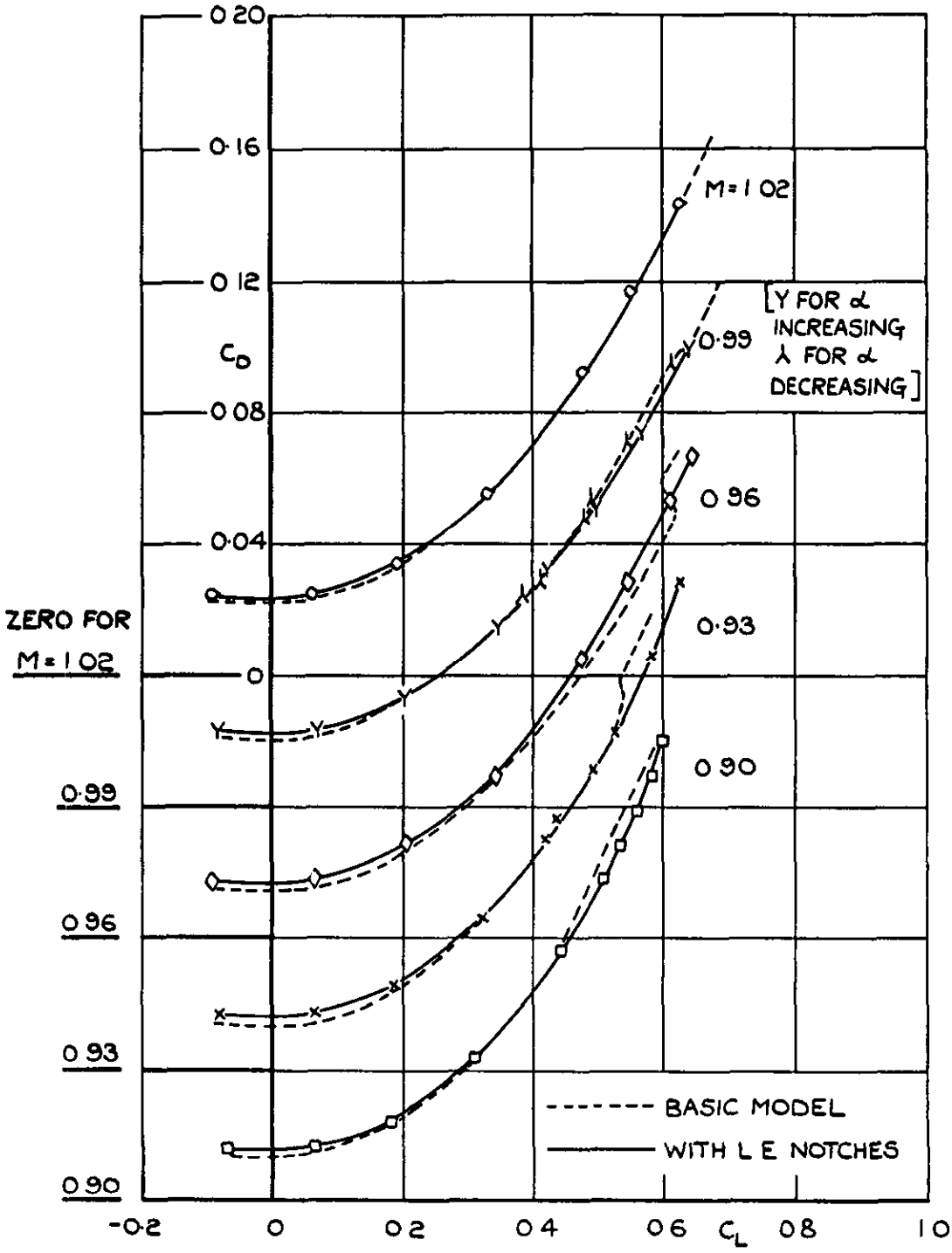

FIG. 8. VARIATION OF C_D WITH C_L FOR MODEL WITH LEADING EDGE NOTCHES ; $\eta = 0$.

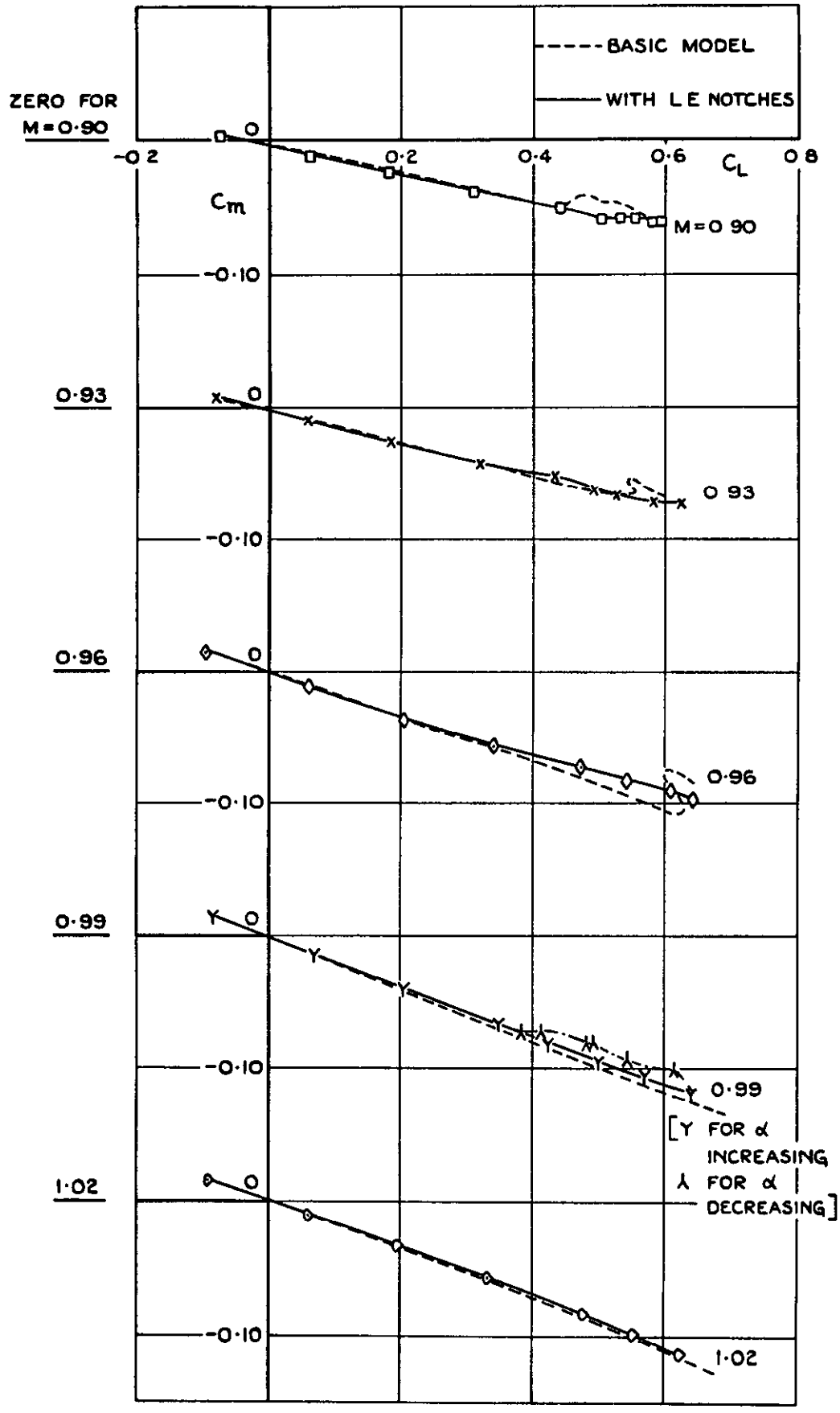

FIG. 9. VARIATION OF C_m WITH C_L FOR MODEL WITH LEADING EDGE NOTCHES ; $\eta = 0$.

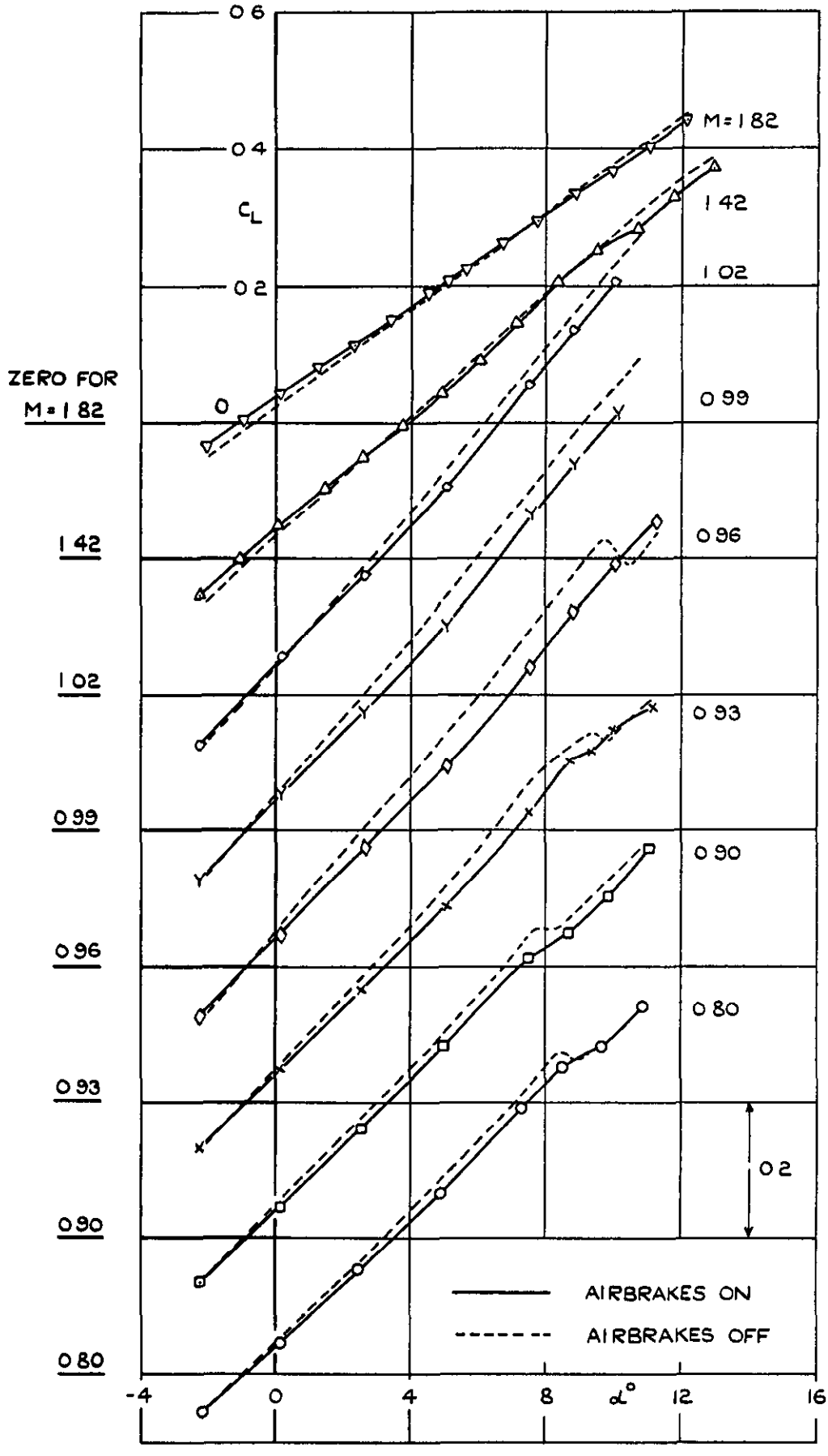

FIG.10(a) VARIATION OF C_L WITH α FOR MODEL WITH AIRBRAKES ; $\eta = 0$.

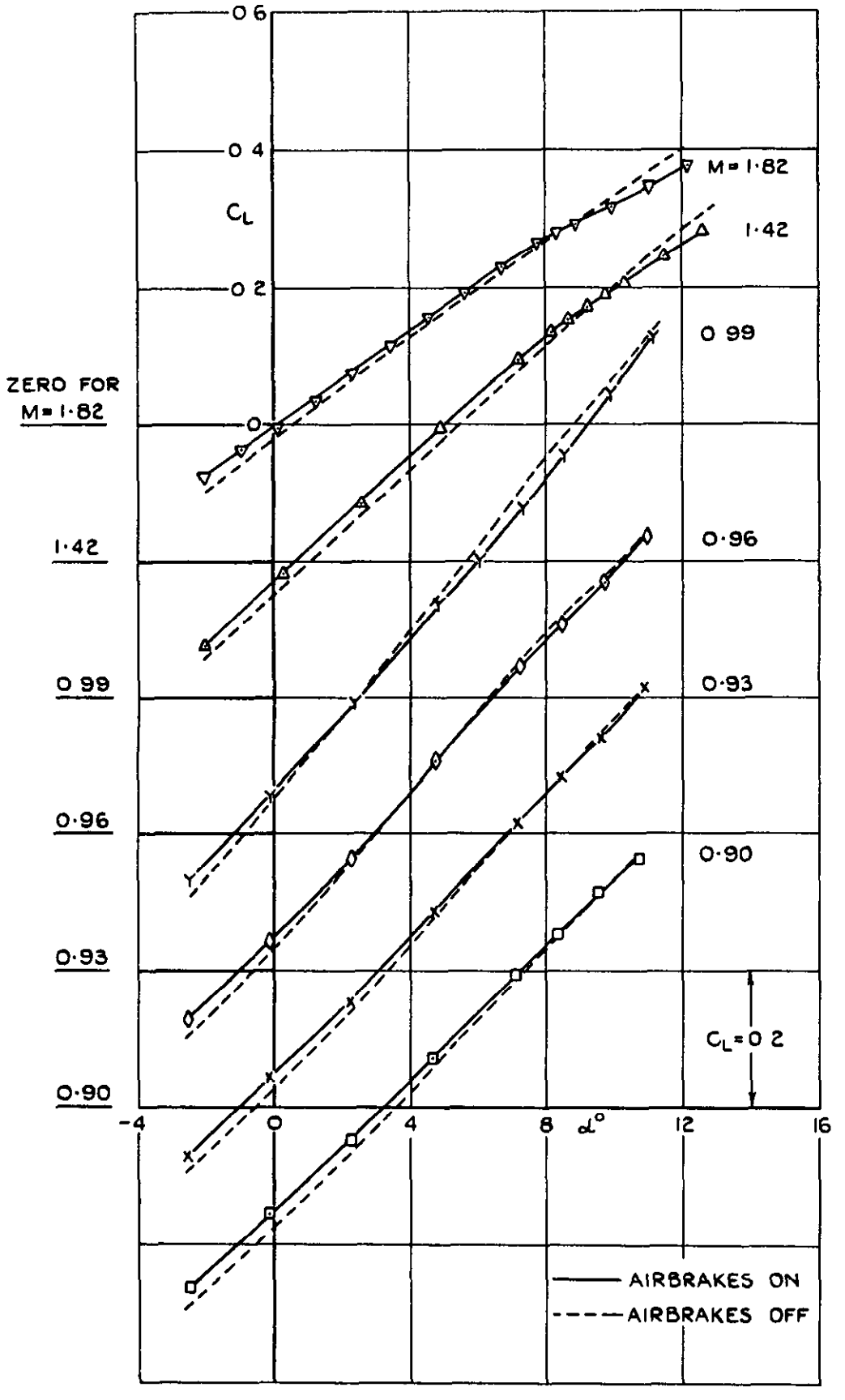

FIG.10(b). VARIATION OF C_L WITH α FOR MODEL WITH AIRBRAKES ; $\eta = -10^\circ$.

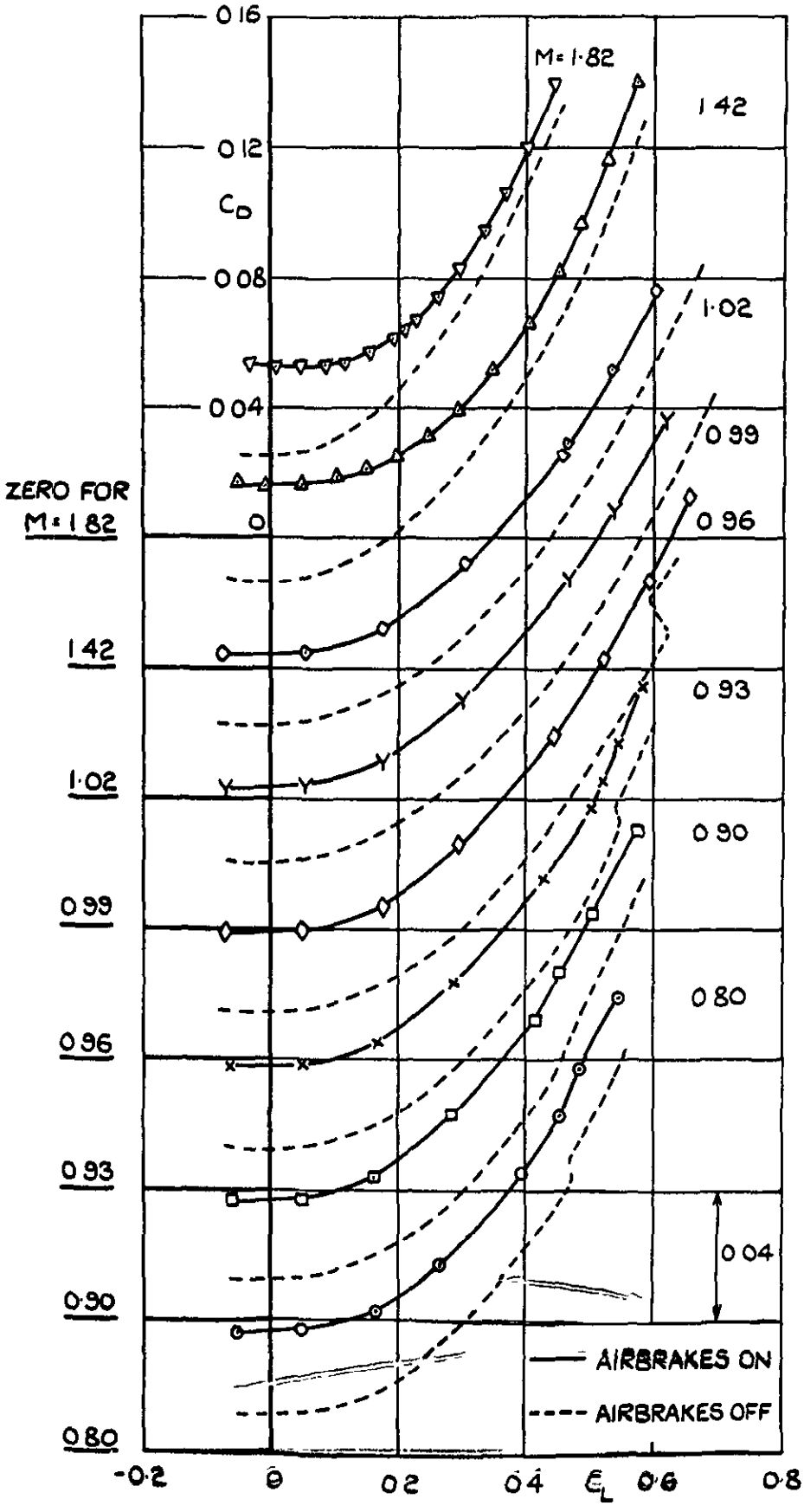

FIG.11(a) VARIATION OF C_D WITH C_L FOR MODEL WITH AIRBRAKES ; $\eta = 0$.

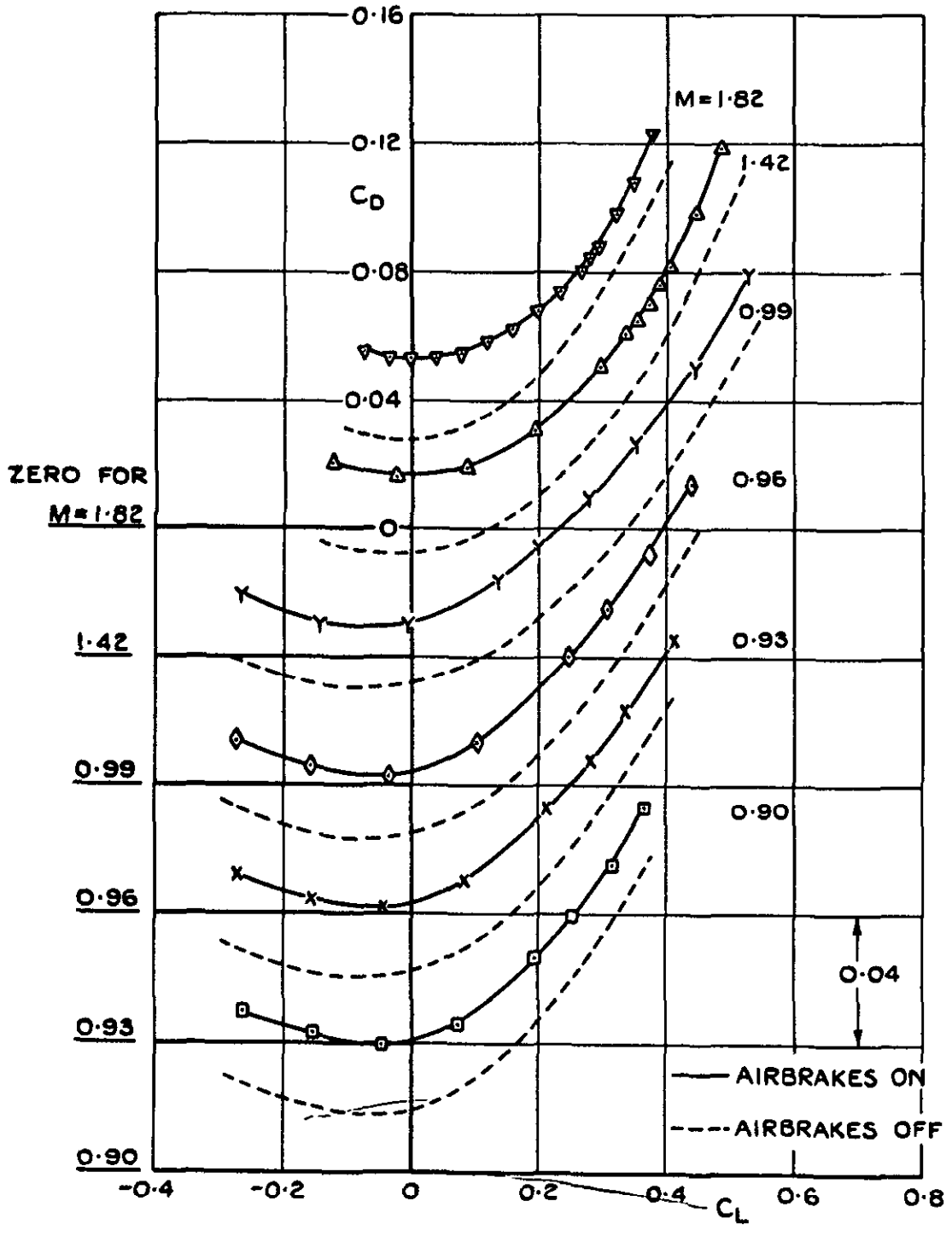

FIG.11(b).VARIATION OF C_D WITH C_L FOR MODEL WITH AIRBRAKES ; $\eta = -10^{\circ}$.

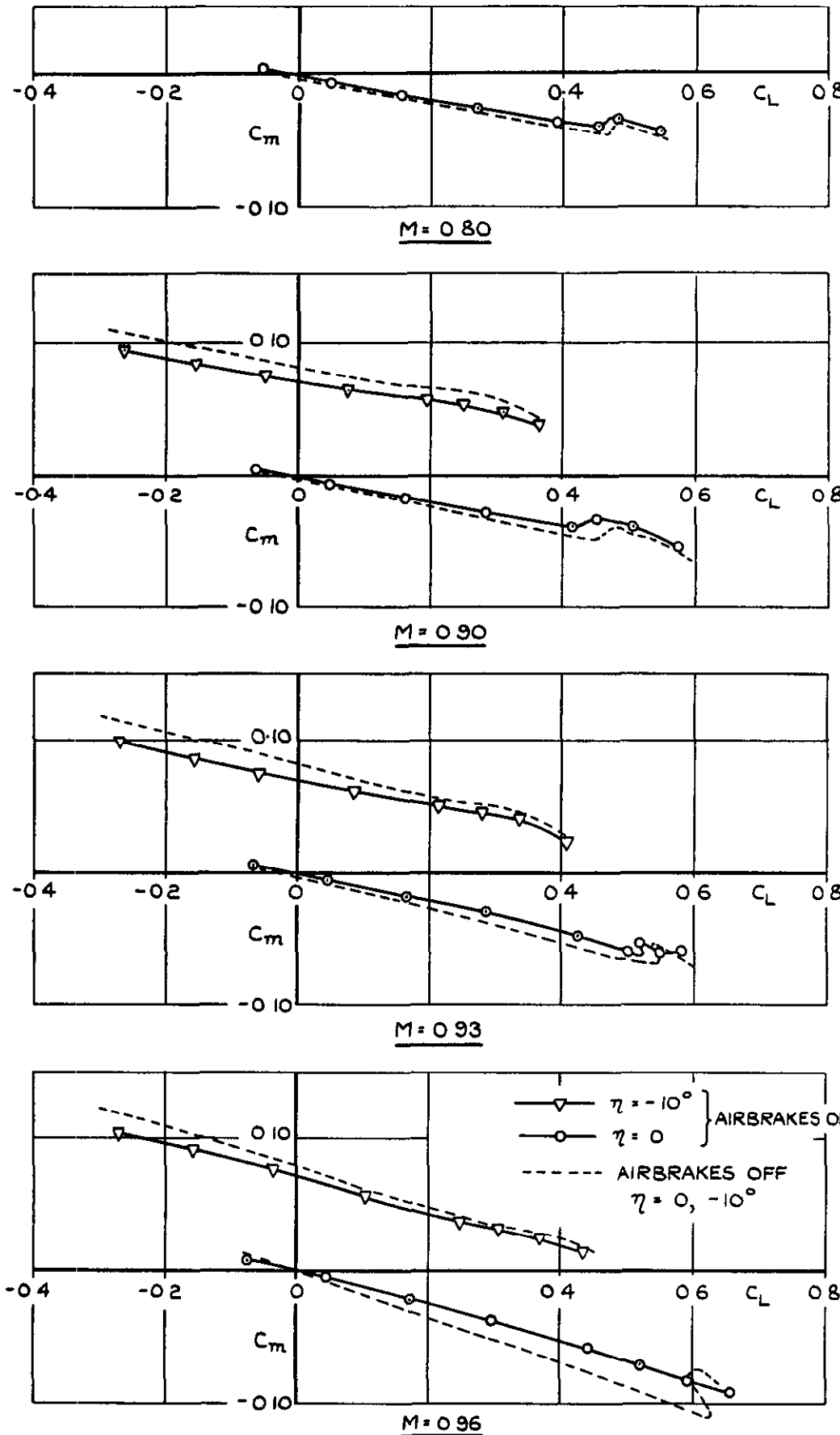

FIG. 12. VARIATION OF C_m WITH C_L FOR MODEL WITH AIRBRAKES ; $\eta = 0$ AND $-10°$

(a) M = 0·80 TO 0·96

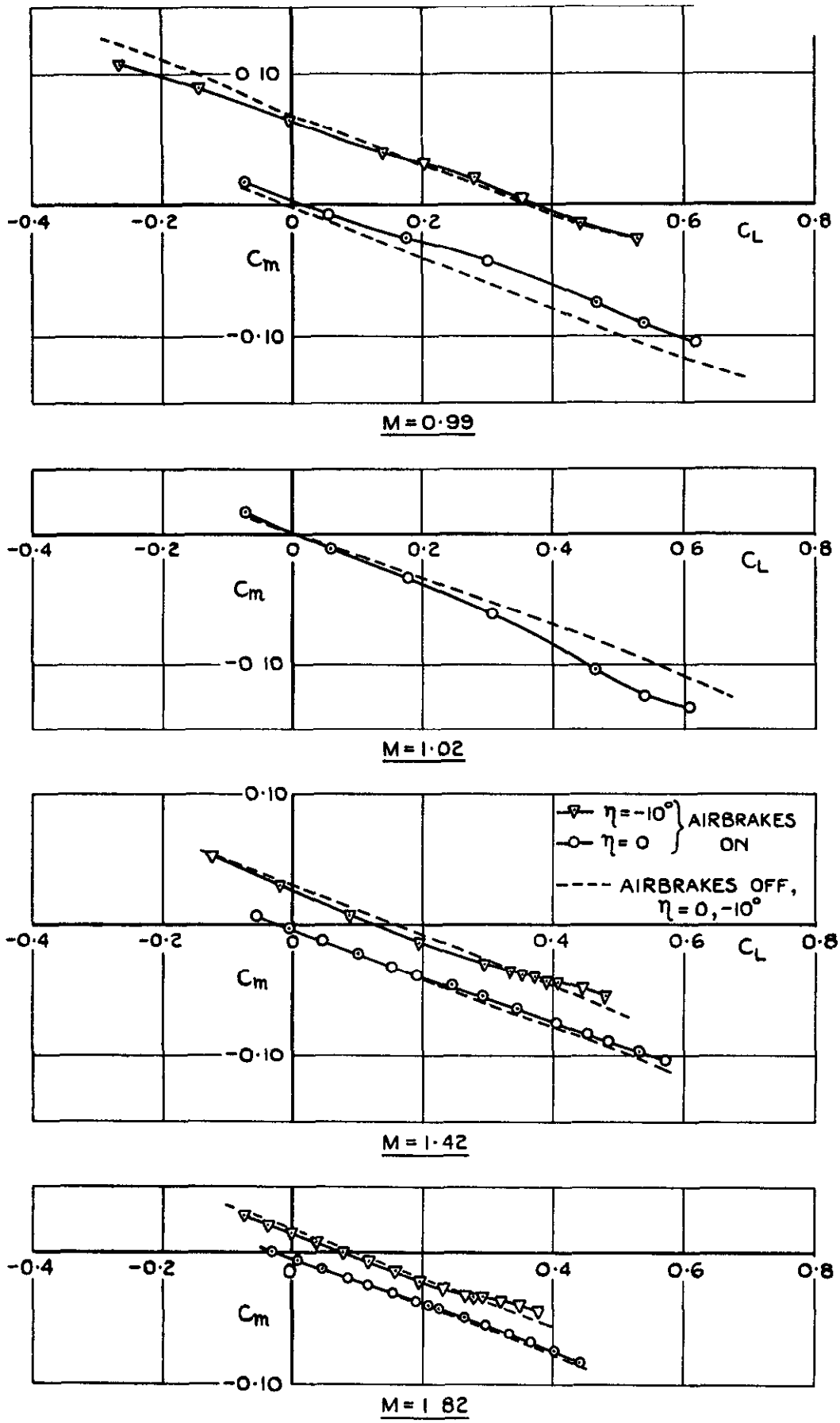

FIG. 12. VARIATION OF C_m WITH C_L FOR MODEL WITH AIRBRAKES.
(b) M = 0·99 TO 1·82.

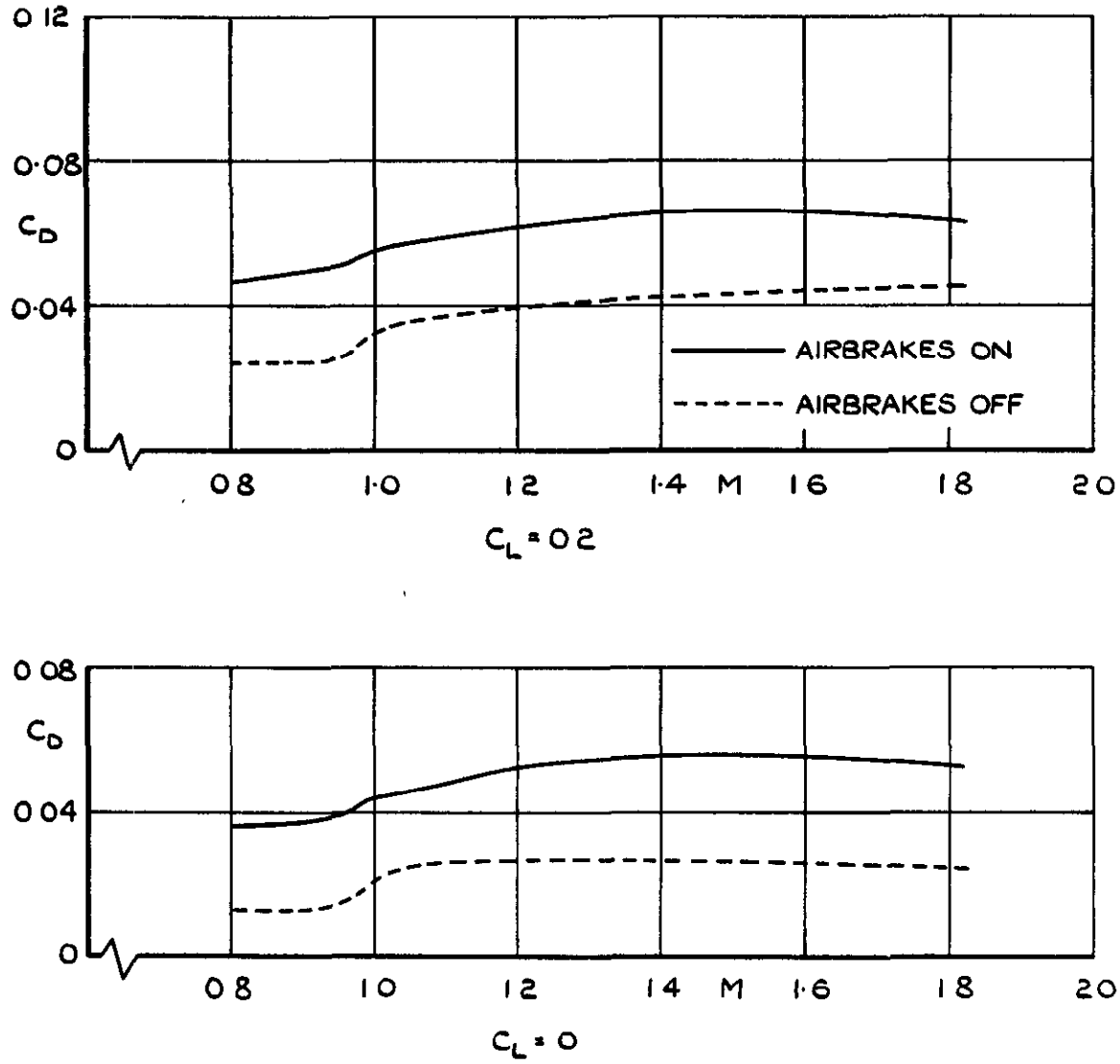

FIG. 13. EFFECT OF AIRBRAKES ON DRAG. VARIATION OF C_D WITH M ; $\eta = 0$.

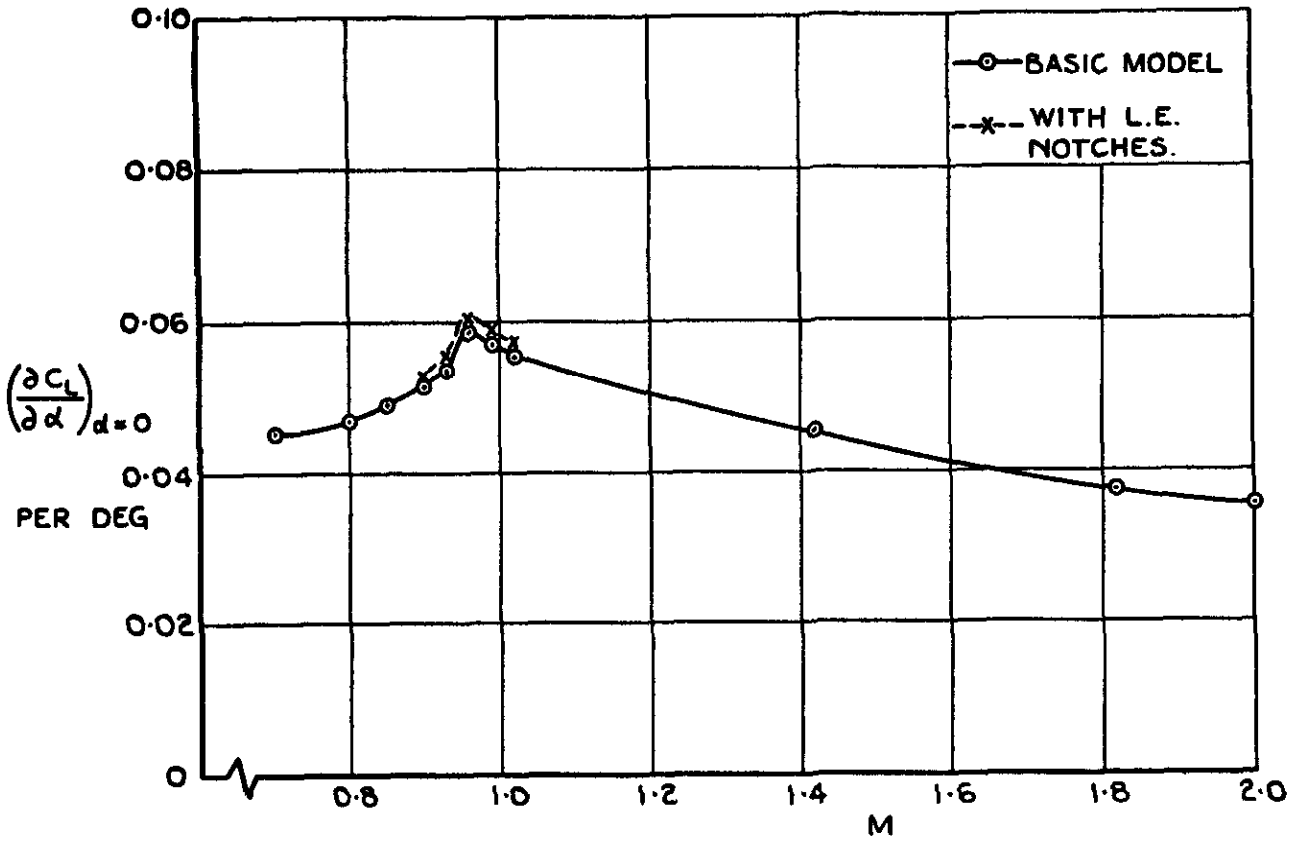

(a) VARIATION OF $[\partial C_L/\partial \alpha]_{\alpha=0}$ WITH MACH No.

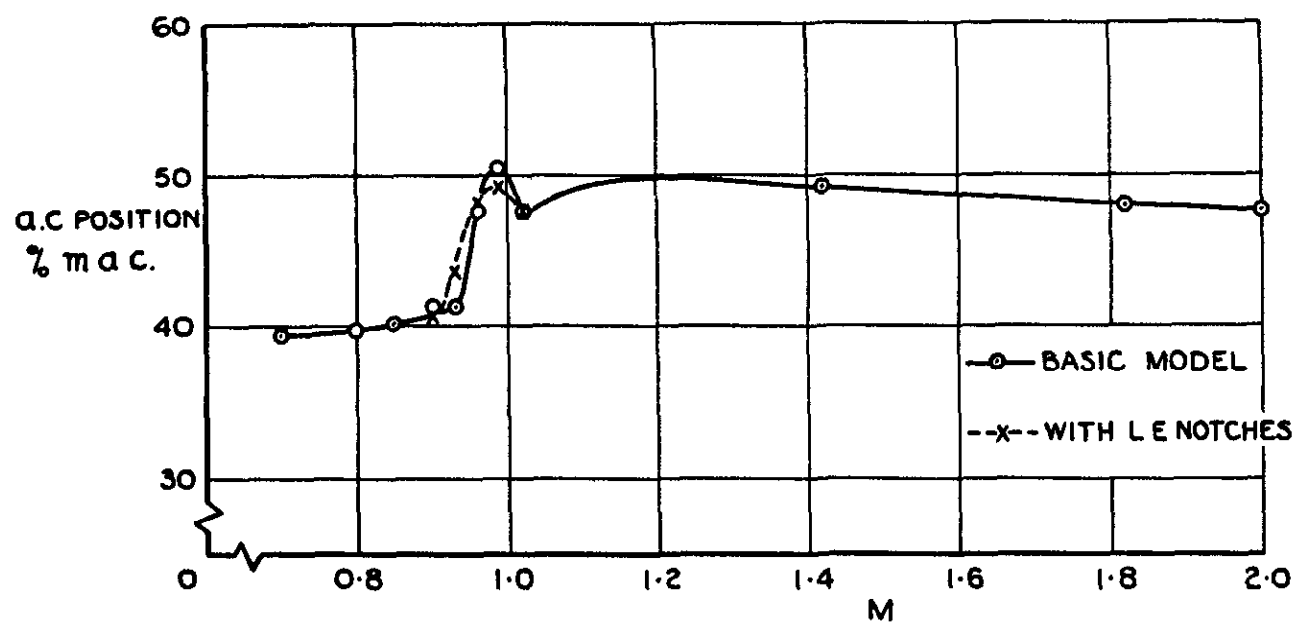

(b) VARIATION OF AERODYNAMIC CENTRE POSITION WITH MACH No.

FIG. 14. BASIC MODEL AND MODEL WITH L.E. NOTCHES ; $\eta = 0$.

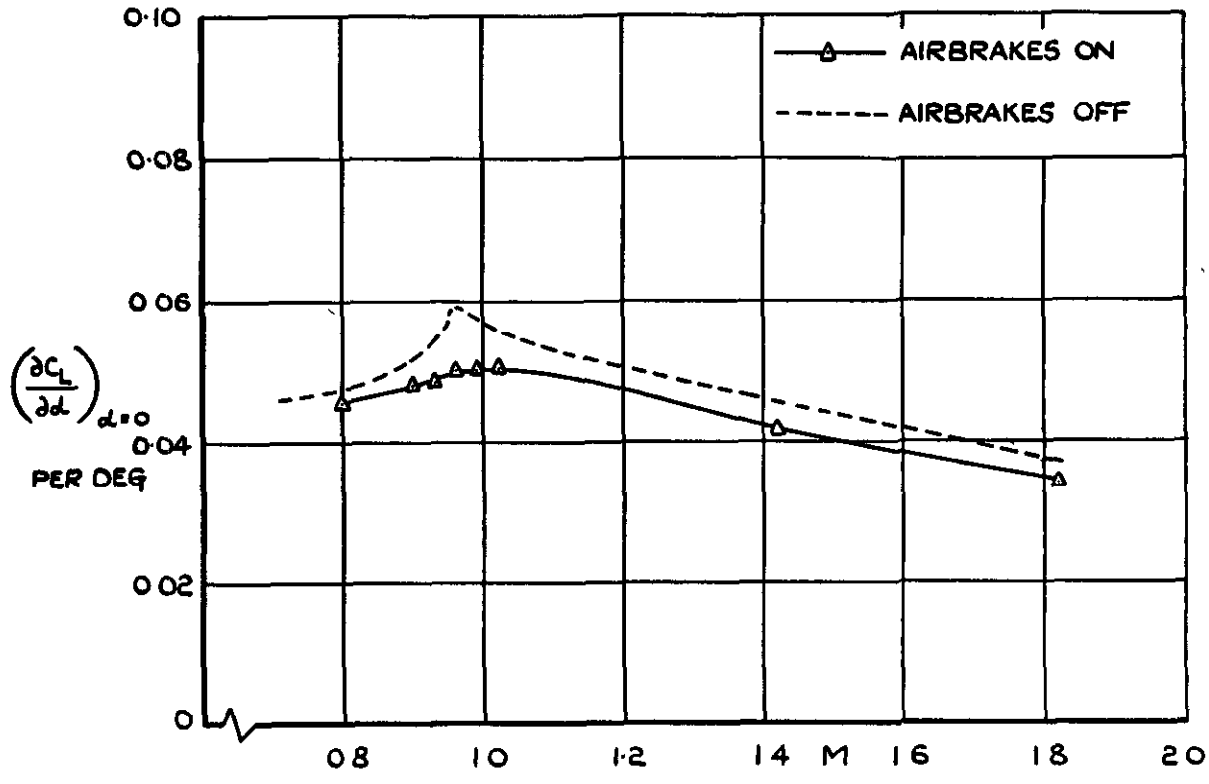

(a) VARIATION OF $[\partial C_L / \partial \alpha]_{\alpha=0}$ WITH MACH No.

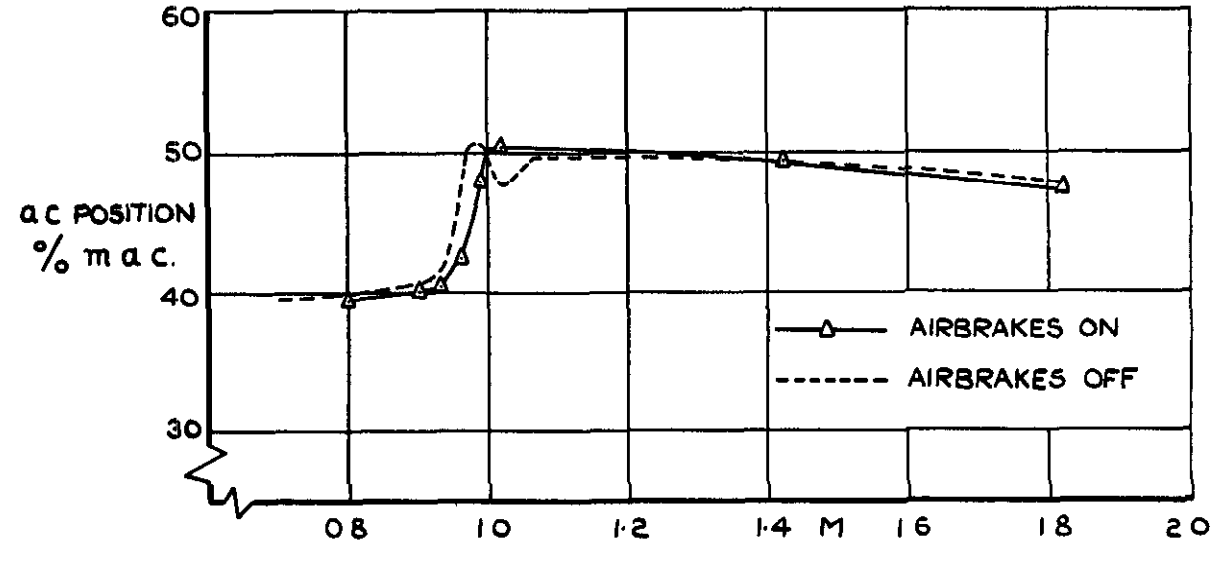

(b) VARIATION OF AERODYNAMIC CENTRE POSITION WITH MACH No.

FIG.15. EFFECT OF AIRBRAKES ; $\eta = 0$.

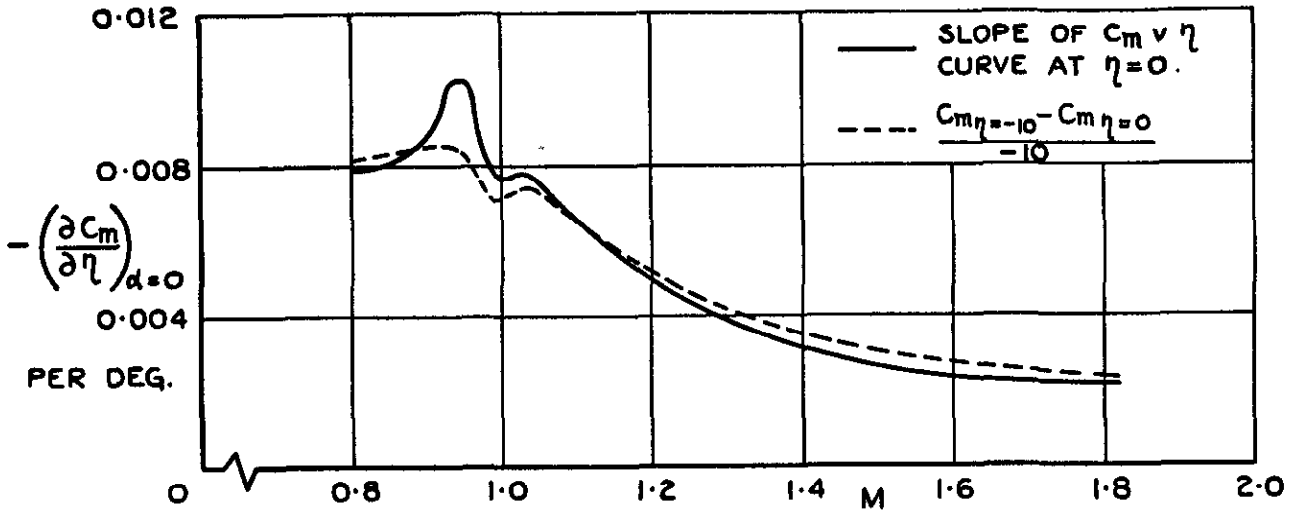

(a) VARIATION OF $-\left(\frac{\partial C_m}{\partial \eta}\right)_{\alpha=0}$ WITH MACH No.

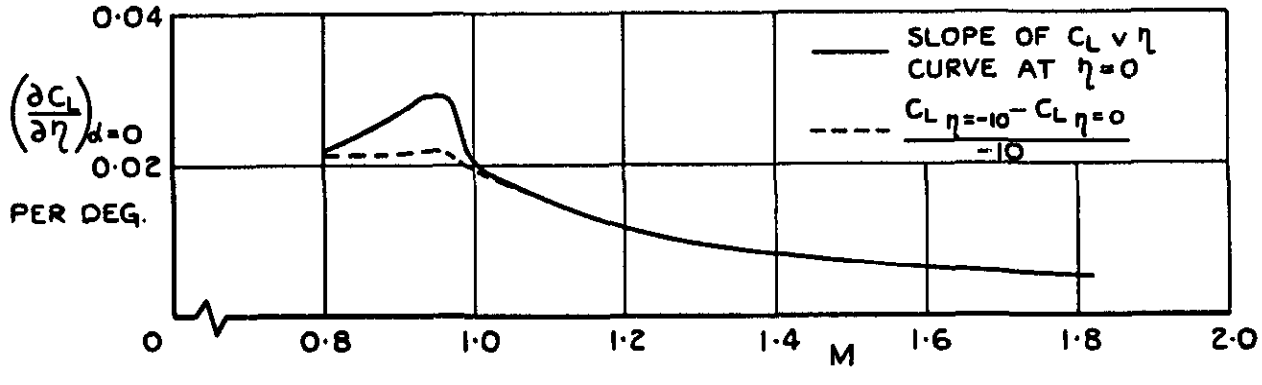

(b) VARIATION OF $\left(\frac{\partial C_L}{\partial \eta}\right)_{\alpha=0}$ WITH MACH No.

FIG. 16. CONTROL EFFECTIVENESS OF BASIC MODEL.

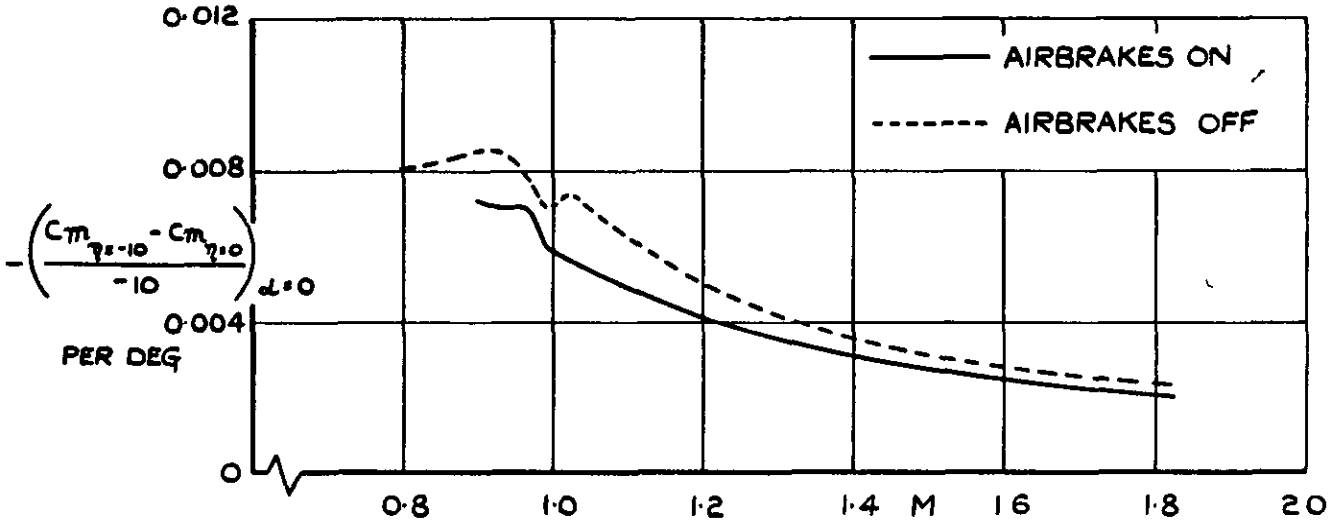

(a) VARIATION OF $-\left(\frac{C_{m_{\eta=-10}} - C_{m_{\eta=0}}}{-10}\right)_{\alpha=0}$ WITH MACH No.

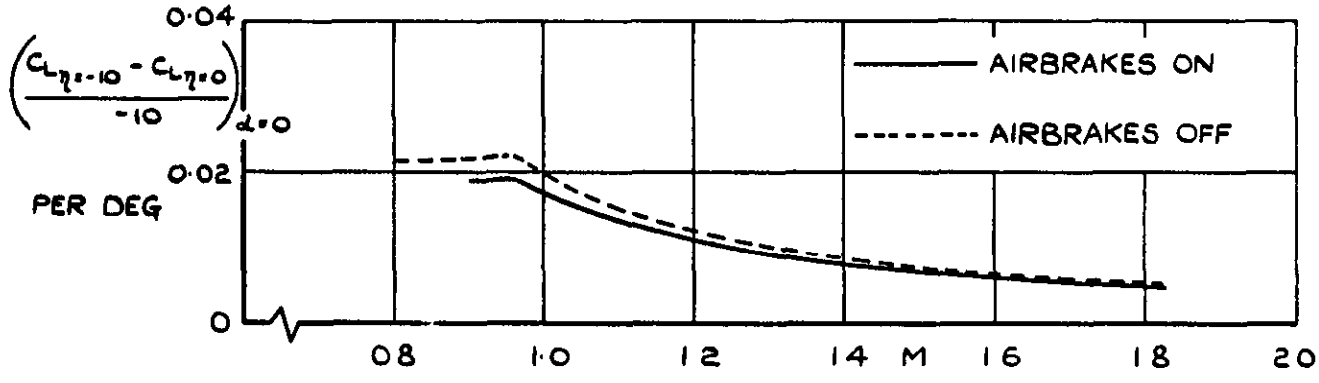

(b) VARIATION OF $\left(\frac{C_{L_{\eta=-10}} - C_{L_{\eta=0}}}{-10}\right)_{\alpha=0}$ WITH MACH No.

FIG.17. EFFECT OF AIRBRAKES ON CONTROL EFFECTIVENESS.

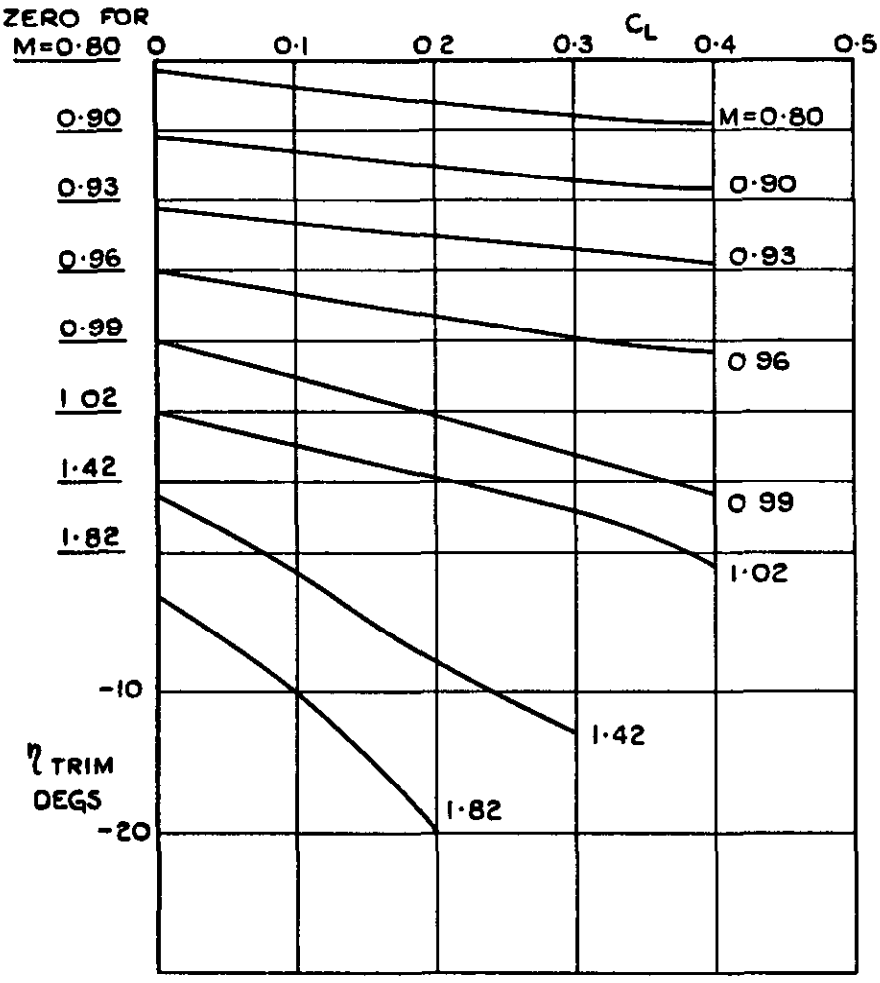

FIG. 18. BASIC AIRCRAFT. VARIATION OF η_{TRIM} WITH C_L.

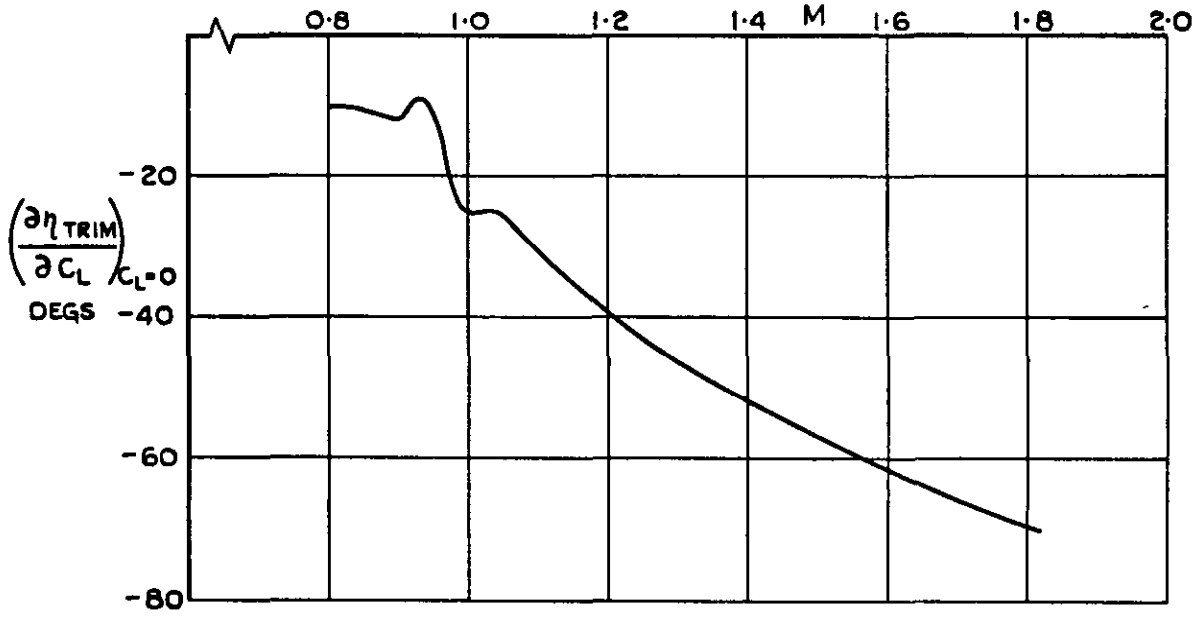

FIG. 19. BASIC AIRCRAFT. VARIATION OF $\left(\frac{\partial \eta_{TRIM}}{\partial C_L}\right)_{C_L=0}$ WITH MACH No.

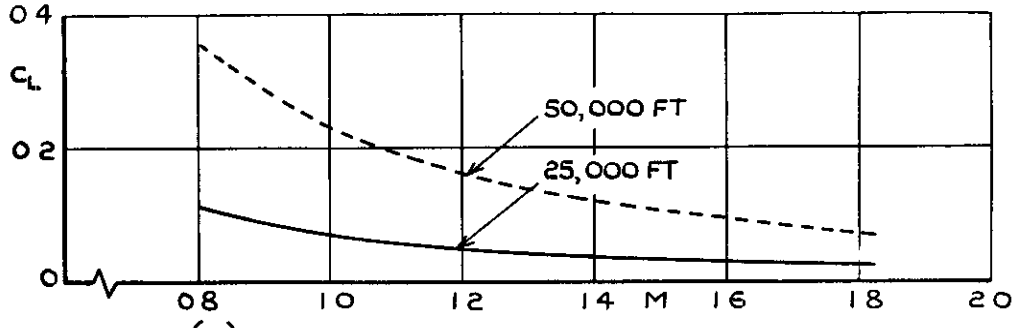

(a) VARIATION OF C_L WITH M

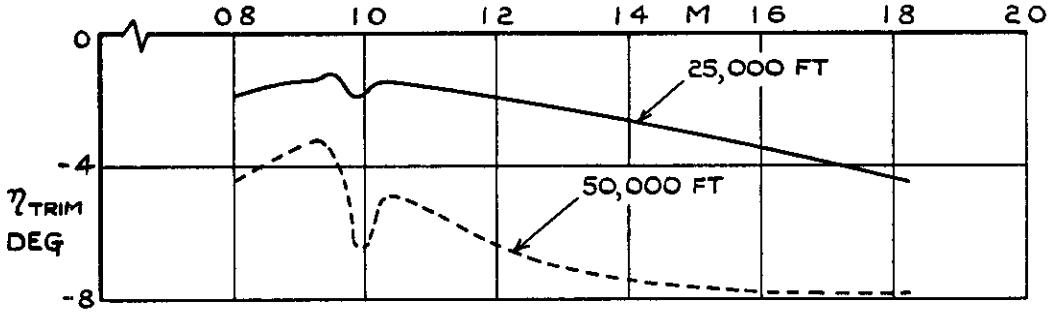

(b) VARIATION OF η_{TRIM} WITH M

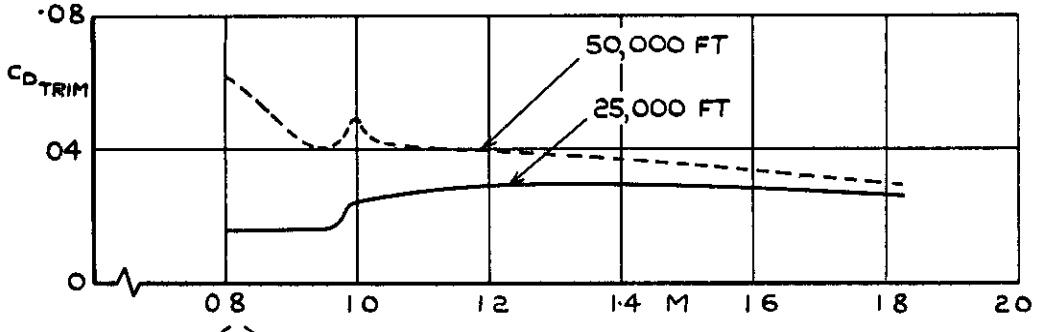

(c) VARIATION OF $C_{D_{TRIM}}$ WITH M

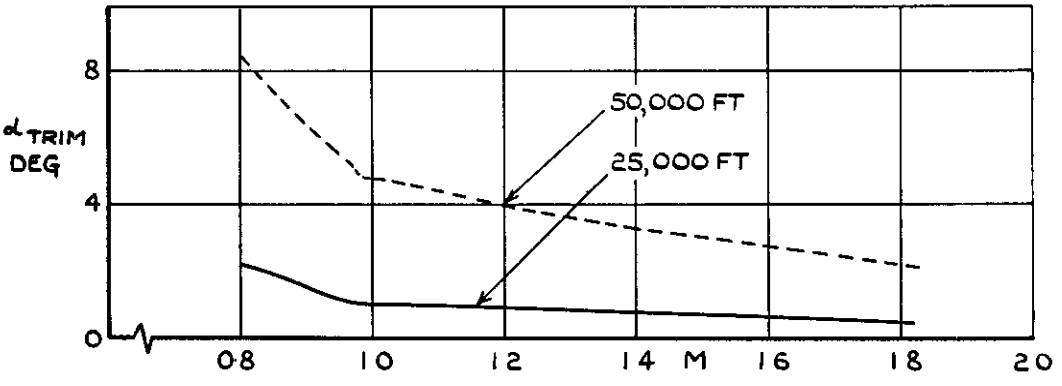

(d) VARIATION OF α_{TRIM} WITH M

FIG. 20. TRIM CHARACTERISTICS OF BASIC AIRCRAFT FOR STRAIGHT AND LEVEL FLIGHT AT 25,000 FT AND 50,000 FT.

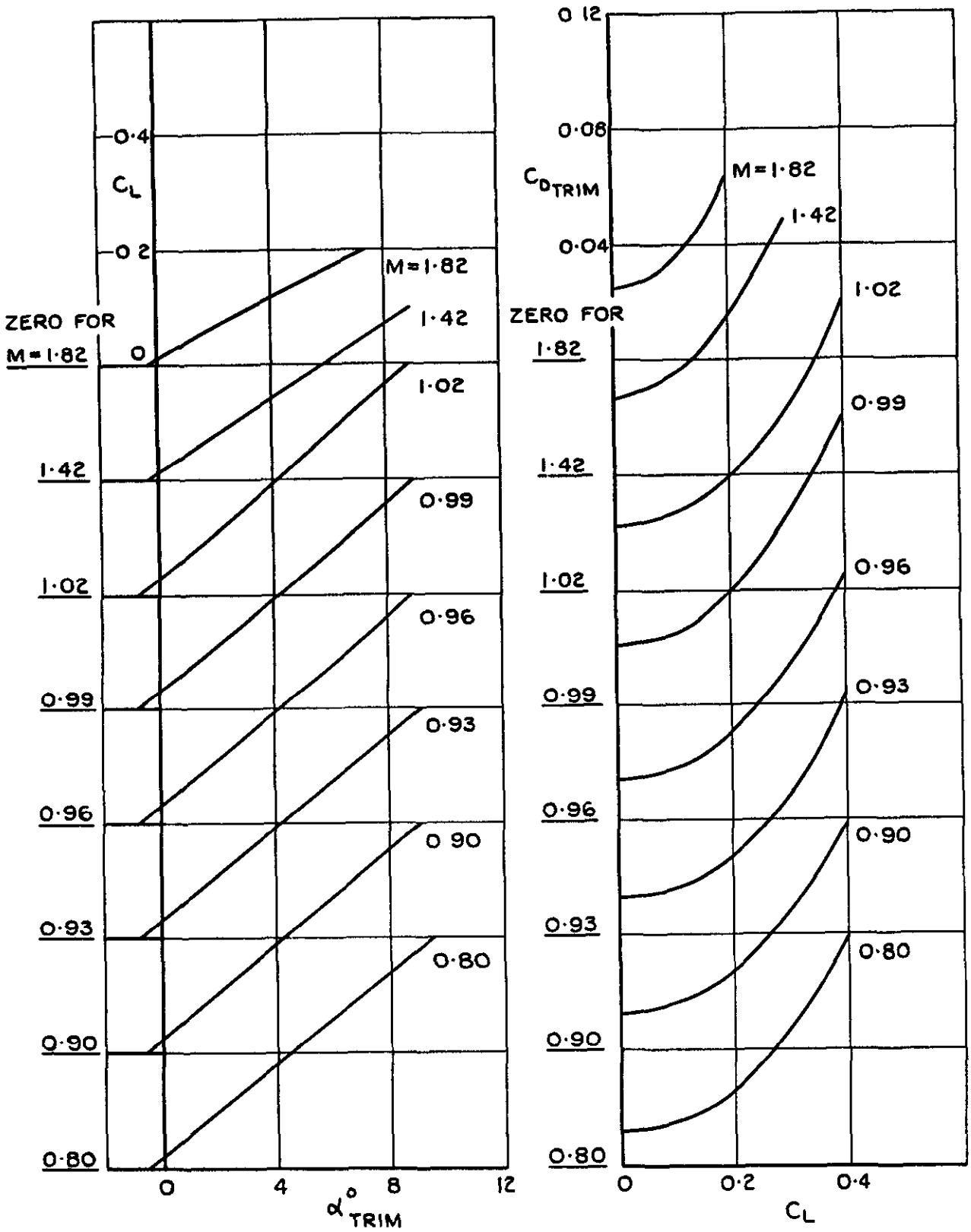

FIG. 21. LIFT AND DRAG CHARACTERISTICS OF TRIMMED AIRCRAFT.

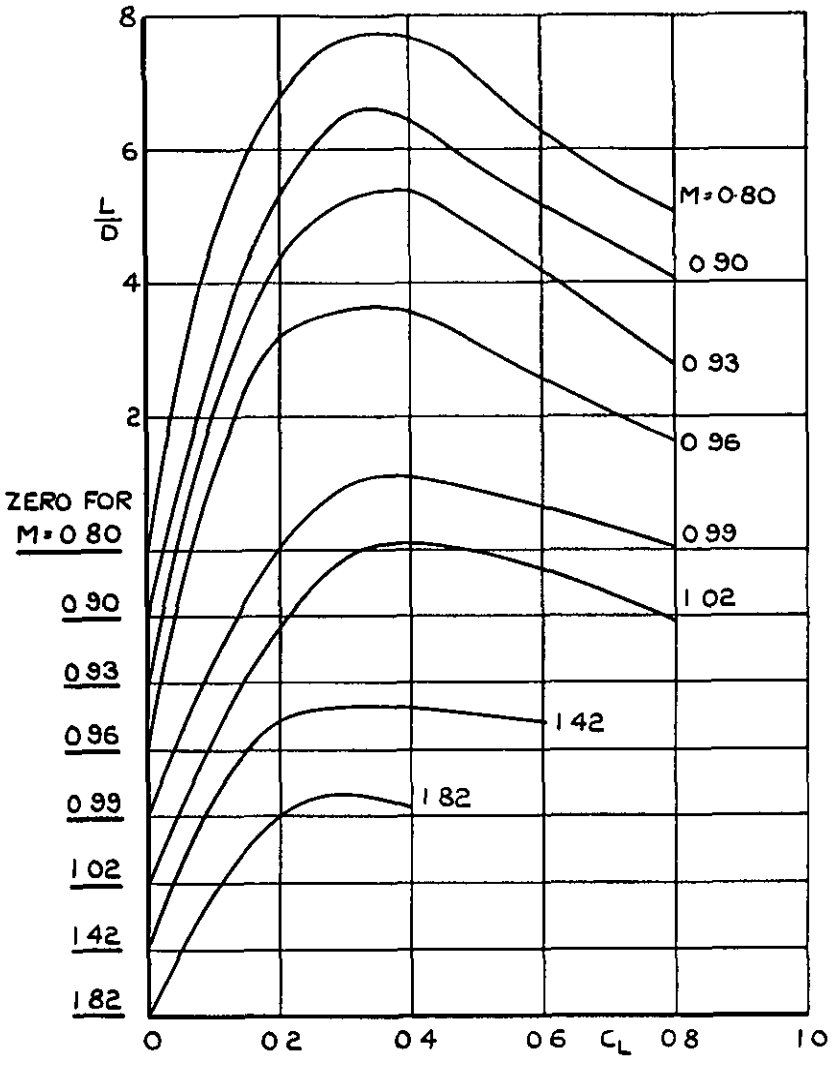

FIG. 22. VARIATION OF L/D RATIOS WITH C_L FOR TRIMMED AIRCRAFT.

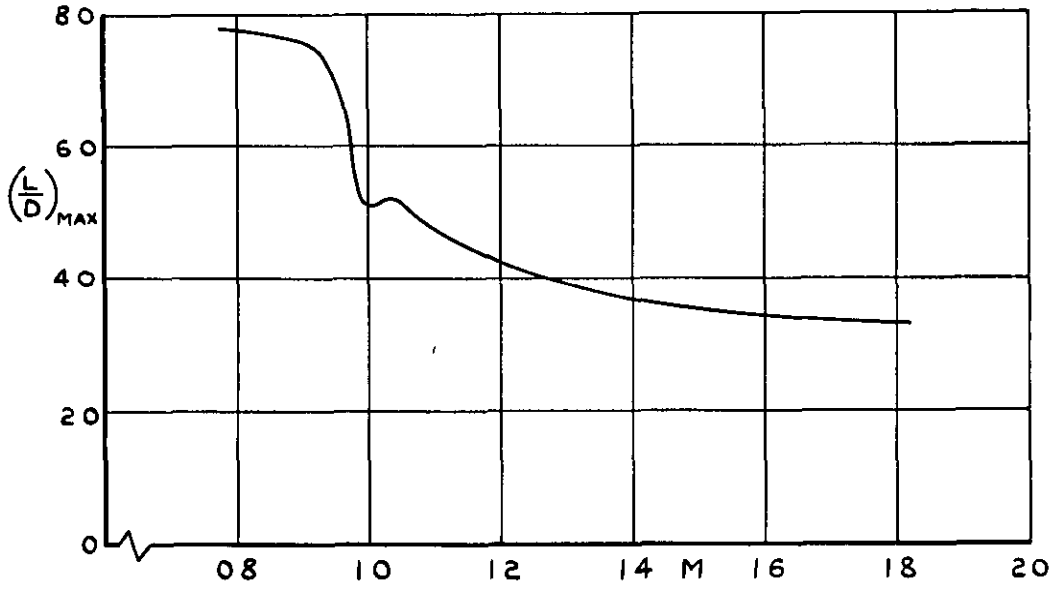

FIG. 23. VARIATION OF $(L/D)_{MAX}$ WITH MACH No. FOR TRIMMED AIRCRAFT.

Printed in England for Her Majesty's Stationery Office by the Royal Aircraft Establishment, Farnborough Dd 501371 K 4

DETACHABLE ABSTRACT CARD

A.R.C. C.P No 1140
May 1960

533.65
533 693 3
533.694.53

Huntley, E.

WIND TUNNEL TESTS AT TRANSONIC AND SUPERSONIC SPEEDS TO INVESTIGATE THE LONGITUDINAL STABILITY OF A MODEL OF THE AVRO 720 AIRCRAFT

1 7.1 2
1 8 1 2 1
1 8.2.1
1 2.2.2.3 1

Tests have been made in the 3ft x 3ft wind tunnel at RAE Bedford on a 1 30 scale model of the AVRO 720 aircraft to investigate the longitudinal stability characteristics at Mach numbers between 0.70 and 2 00. Additional tests were made with airbrakes attached to the rear-fuselage and with notches cut in the leading edges of the wing at 66.7% semispan

The results show no doubtful features apart from a sharp but small transient pitch-up at lift coefficients around $C_L = 0\,45$ for $M = 0\,80$ and $C_L = 0\,60$ for $M = 0\,96$ The instability is appreciably reduced by the application of up-elevon and is almost completely eliminated by the leading edge notches. The notches, however, introduce some instability at M = 0.99 where none had occurred originally

A.R C. C.P No 1140
May 1960

533 65
533 693 3
533 694 53

Huntley, E.

WIND TUNNEL TESTS AT TRANSONIC AND SUPERSONIC SPEEDS TO INVESTIGATE THE LONGITUDINAL STABILITY OF A MODEL OF THE AVRO 720 AIRCRAFT

1 7 1 2
1 8 1 2 1
1 8 2.1
1.2 2.2.3.1

Tests have been made in the 3ft x 3ft wind tunnel at RAE Bedford on a 1 30 scale model of the AVRO 720 aircraft to investigate the longitudinal stability characteristics at Mach numbers between 0 70 and 2 00 Additional tests were made with airbrakes attached to the rear-fuselage and with notches cut in the leading edges of the wing at 66 7% semispan.

The results show no doubtful features apart from a sharp but small transient pitch-up at lift coefficients around $C_L = 0\,45$ for $M = 0\,80$ and $C_L = 0\,60$ for $M = 0\,96$ The instability is appreciably reduced by the application of up-elevon and is almost completely eliminated by the leading edge notches. The notches, however, introduce some instability at M = 0 99 where none had occurred originally

Published by
HER MAJESTY'S STATIONERY OFFICE

To be purchased from
49 High Holborn, London WC1 V 6HB
13a Castle Street, Edinburgh EH2 3AR
109 St Mary Street, Cardiff CF1 1JW
Brazennose Street, Manchester M60 8AS
50 Fairfax Street, Bristol BS1 3DE
258 Broad Street, Birmingham B1 2HE
80 Chichester Street, Belfast BT1 4JY
or through booksellers

C.P. No. 1140

SBN 11 470388 4